



Late Aptian carbonate platform evolution and controls (south Tethys, Tunisia): response to sea-level oscillations, palaeo-environmental changes and climate

Najeh Ben Chaabane¹ · Fares Khemiri² · Mohamed Soussi¹ · Illef Belhaj Taher²

Received: 4 March 2021 / Accepted: 27 July 2021 / Published online: 16 August 2021
© Springer-Verlag GmbH Germany, part of Springer Nature 2021

Abstract

The late Aptian Lower Serdj Formation (LSF) in the Northern Atlas of Tunisia records a mixed carbonate–siliciclastic system from the southern margin of Tethys. Sedimentological investigations of key sections in the Serdj-Bargou area along a NE–SW-platform-to-basin profile reveal five shallow-marine carbonate units (Cu1, Cu2, Cu3, Cu4a and Cu4b), dominated by subtidal deposits, separated by four terrigenous units (T1, T2, T3, T3a). Twelve basic facies are grouped into six facies associations or zones (FZA to FZF), representing particular palaeo-environments from proximal to distal settings. Carbonate units Cu1, Cu2 and Cu4a are dominated by coral algal-*Orbitolina* facies representative of a homoclinal ramp. However, units Cu3 and Cu4b are dominated by high-energy oolitic facies of a shoaled ramp. The terrigenous deposits (T1 to T4) are dominated by siliciclastics with shale, sandstone/siltstone and marl and have mostly been assigned to off-platform to basinal environments (FZF). The vertical facies changes are closely related to amplitudes of sea-level fluctuations and late Aptian Tethyan climatic perturbations. The terrigenous units were the result of short cooling periods and a humid climate. Moreover, this climate favoured the development of tide-influenced oolitic shoals, with the nuclei of ooids formed by fine quartz grains. Both the oolitic and siliciclastic deposits reflect episodes of maximum platform progradation basin-ward at a time of low accommodation space through the late Aptian period. Overall the new stratigraphic dataset from the southern Tethys margin is interpreted as reflecting the global Late Aptian cooling episode and sea-level lowstand.

Keywords Late Aptian · Carbonate platform · Sea level · Climate · South Tethys · Central Tunisia

Introduction

The determination of carbonate platform types, their facies heterogeneities, their internal architecture, and spatio-temporal evolution is complex because of the multiple controlling factors. The resolution of these complexities is possible based on field data and detailed stratigraphic and sedimentological investigations. Each platform succession has a distinctive and unique character that responds to the tectonic context, and climatic, physical, chemical and biological

conditions of its Phanerozoic time-interval (Pomar 2001; Pomar and Hallock 2008).

During the Mesozoic period, Tunisia (southern Tethys) was the site of shallow-water carbonate deposits (e.g. Jurassic: Soussi 2002; Early Cretaceous: Tlatli 1980; M'Rabet 1981; Masse 1984; Heldt et al. 2010; Hfaiedh et al. 2013 and Late Cretaceous: Tourir et al. 1989; Negra et al. 2016). During the late Aptian to early Albian period, the Serdj-Bargou area (Central Tunisia) consisted of a tropical epicontinental sea, dominated by shallow-marine carbonate facies of the Serdj Formation (Tlatli 1980; Heldt et al. 2010; Ben Chaabane 2019). It is one of the best developed carbonate platforms (Fig. 1) recorded around the Tethys ocean (e.g. Heldt et al. 2010; Ben Chaabane et al. 2019; Ben Chaabane 2019). The Lower Serdj Formation stratal units (Fig. 1c) and their internal organization were influenced by relative sea-level change, accommodation space availability, carbonate production, ecological conditions and regional climate change (Tlatli 1980; Ben Chaabane et al. 2013, 2019).

✉ Najeh Ben Chaabane
najeh.benchaabane@fst.utm.tn; najeh.geo.tun@live.fr;
najeh.benchaaban@fst.utm.tn

¹ Faculty of Sciences, Department of Geology, University of Tunis El Manar, LR18ES07, P. C, 2092 Tunis, Tunisia

² Tunisian Oil Company (ETAP), 54 Street Mohamed V, 1002 Tunis, Tunisia

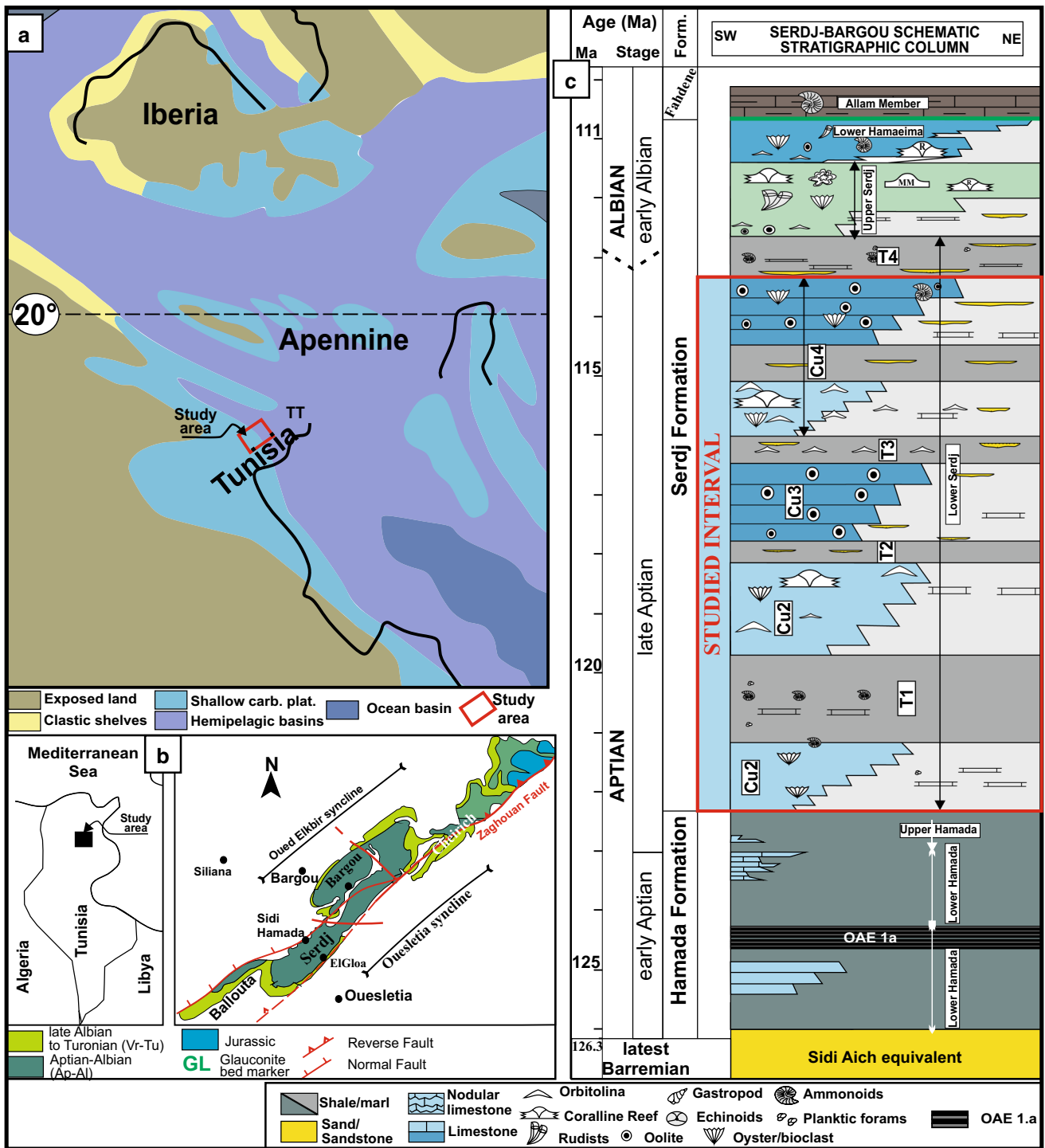


Fig. 1 **a** Global palaeogeographic map during the early Cretaceous (120 Ma), **b** Simplified geographic and geological maps of the study area showing the Tunisian ridge “dorsale tunisienne” structural domain and the main tectonic features of the Sedj-Bargou-Zaghouan structure. It consists of faulted folds bounded by the NE–SW Zagh-

ouan major reverse fault. The Sedj-Bargou anticlinorium bordered to the north by the Oued Elkebir syncline and to the south by the Ouesletia syncline. **c** Schematic stratigraphy and the main sedimentary events of the Aptian–Lower Albian of northern Atlas Tunisia (Serdj-Bargou area)

The Hamada Formation and Lower Serdj Formation represent an early to late Aptian second-order regressive cycle (Hardenbol et al. 1998; Catuneanu et al. 2011;

Catuneanu 2019; Ben Chaabane et al. 2019). Furthermore, the Lower Serdj (upper Aptian) comprises several third-order transgressive/regressive sequences (Sarg 1988; Haq

et al. 1988; Ben Chaabane et al. 2019). Both second- and third-order cycles were affected by the creation and suppression of accommodation space from the early to late Aptian. Moreover, several authors have interpreted eustatic sea-level oscillations as a response to an early Cretaceous global greenhouse climate interrupted during the late Aptian by short cold phases (e.g., Pomar and Kendall 2008; Van Buchem et al. 2010; Heldt et al. 2010; Bonin 2011; Maurer et al. 2013; Millán et al. 2011; Bover-Arnal et al. 2014; Skelton et al. 2019).

This paper focuses on the upper Aptian deposits, the Lower Serdj Formation (LSF), at Jebel Serdj-Bargou (sensu Ben Chaabane et al. 2019). Herein, the LSF consists of five carbonate units (Cu1, Cu2, Cu3, Cu4a, and Cu4b) separated by four terrigenous units (T1 to T4). The calcareous grains of these carbonate units are ooids, orbitolinids, corals and bivalves (rudist and oyster debris), as well as other benthic foraminifers. This diversity was triggered by several factors including carbonate saturation state, trophic and oxygen levels, light and bathymetry during sedimentation (Fischer and Arthur 1977; Hallock and Schlager 1986; Riding 2002; Riding and Liang 2005).

The present paper focuses on the reconstruction of the principal evolutionary carbonate stages and their associated palaeo-environments of the upper Aptian strata cropping out in the Serdj-Bargou domain (Central Tunisia). This study will concentrate, essentially, on the Lower Serdj carbonate units. The main carbonate grains and facies in the Lower Serdj Formation and its lateral equivalents will be described and interpreted. Furthermore, the tectonic control on sea-level oscillations and the possible impact

of siliciclastic input on late Aptian sedimentation will be discussed.

Several studies have documented a pronounced global regression in the last half of the late Aptian (e.g. Maurer et al. 2013; Bover-Arnal et al. 2016). These changes are recognized in several tectonic plates and led to widespread erosion and terrigenous sedimentation. However, in Tunisia, the late Aptian terrigenous runoff is poorly documented and not well understood. Thus, understanding the stratigraphic evolution of the LSF units and the timing of alternating carbonate and terrigenous clastic facies will provide information on the palaeo-environment and climatic changes.

Setting

Regional setting and stratigraphy

During the Early Cretaceous, Tunisia was part of a passive margin on the northern periphery of the African continent and situated along the southern Tethyan domain (Masse et al. 1993). Central Tunisia displays widespread facies of shallow-marine environments from this time. These environments were continuous with the well-known carbonate platform (Fig. 1a) that developed around much of the Tethyan margin and the Arabian plate during this time (e.g., Van Buchem et al. 2010; Bover-Arnal et al. 2016; Skelton et al. 2019).

During the Aptian to early Albian, the Tunisian Northern Atlas (Serdj-Bargou domain) stratigraphy records three important episodes (Ben Chaabane et al. 2019), with clear lithofacies contrasts (Fig. 2). They are, respectively

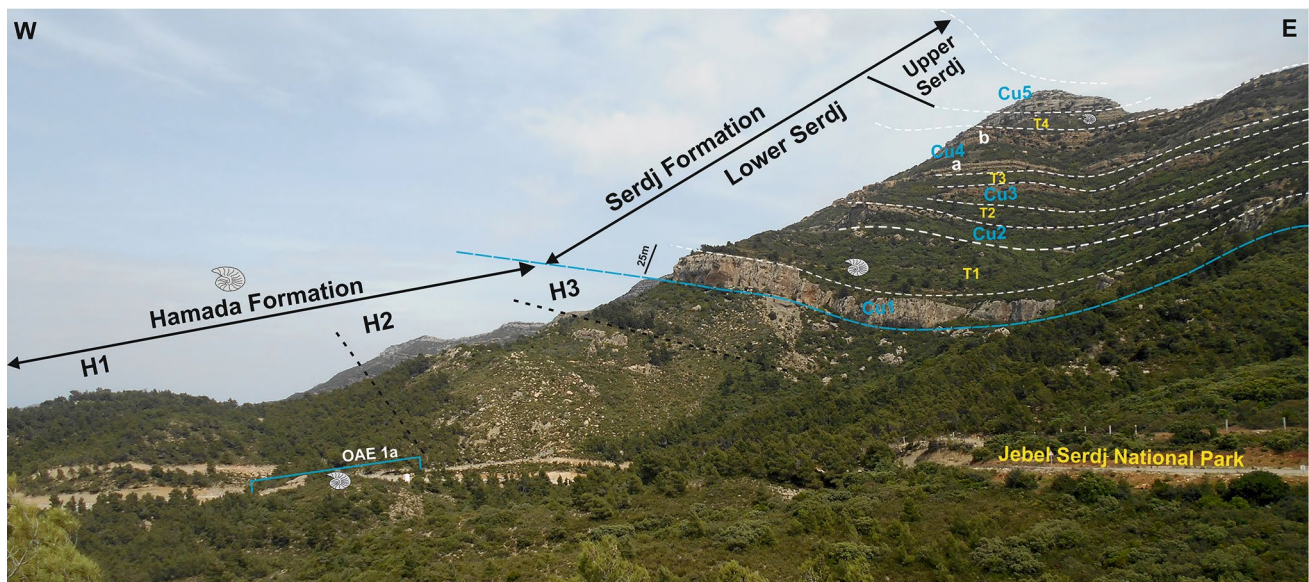


Fig. 2 Panoramic view of the SH section (Serdj Formation stratotype) with the different stratigraphic units of the Aptian–early Albian period: (1) the lower part represented by the Hamada Formations

(H1, H2 and H3) and the upper part showing the Serdj Formation (Lower and Upper Serdj)

(1) the Hamada Formation, dominated by shale and marl, including in the lower part the sedimentary record of OAE 1a (early Aptian to lowermost late Aptian), (2) the second episode (late Aptian), characterized by shallow-marine carbonate units (Cu1, Cu2, Cu3, and Cu4) separated by marly/terrigenous units (T1, T2, T3, and T4), all of which are in the Lower Serdj Formation (LSF), the focus of this study, and (3) the last episode represented by the Upper Serdj Formation that documents a net change in sedimentation to widespread shallow-marine carbonates with corals, rudists and benthic foraminifera (early Albian). The uppermost Aptian (LSF) deposits consist of platform-to-basin environments (Ben Chaabane 2019) with five shallow-water carbonate units. Laterally, a substantial stratigraphic thinning is evident with the lateral facies changes (Fig. 4).

Geographic and geological settings

The Serdj-Bargou area is located in Central Tunisia, near Bargou village (Fig. 1b). It exposes one of the most complete upper Aptian successions recognized in Central Tunisia (Fig. 1); thus, it can provide new information on the southern Tethys realm. Furthermore, it offers the opportunity to analyse the most basin-ward advanced position of the late Aptian carbonate platform facing the Tunisian Trough “Sillon tunisien” (TT: Fig. 1a).

All of the studied sections are located on the Serdj-Bargou (SB) mega-anticlinorium. It belongs to a structural domain called in local nomenclature “la Dosale Tunisienne” (Figs. 1b, 3). It is dominated by NE-SW trending faulted folds transected by NW-SE to E-W faults (Turki 1985). This anticlinorium is delimited on the NW by the Oued El Kebir syncline and on the SE by the Ousseletia syncline (Figs. 1, 3). In this area, the Aptian to early Albian period is represented by two formations: the deep-marine Hamada and the dominantly shallow carbonate Serdj Formation (Ben Chaabane et al. 2019). The LSF overlies planktic foraminifer-rich deep-marine shales (Fig. 1c) of the upper Hamada Formation (H3) and is capped by transgressive ammonite-rich deposits of the fourth terrigenous unit (Figs. 1, 4). The Lower Serdj (LS) Formation is significant in terms of understanding the late Aptian Tethyan climate.

Dataset and methods

Six sedimentological sections were logged bed-by-bed and sampled along a 20 km-long profile of the Serdj-Bargou mountains (Fig. 3). These sections are, respectively, from SW to NE: (2) Beskra Kef Hassan (KH-BS); (3) Al-Ghamaylia

(AG); (1) Sidi Hamada (SH/SR); (4) Bir Attay (BT); (5) Kef Lahmar (KL), and (6) Oued Drija (OD).

Microfacies analysis was performed on over 300 thin sections to identify the main grains (skeletal/non-skeletal), matrix and textures (Dunham 1962 modified by Klovan 1971) and to define the facies associations based on the abundance and arrangement of these grains. The presence/absence of ooids and coral enables the different stages of the LSF platform to be distinguished (Fig. 3). 12 elementary facies and 6 Facies Zones (FZ) have been identified that represent particular depositional settings (Dunham 1962 modified by Klovan 1971; Wilson 1975; Read 1995; Flügel 2010). The palaeo-environmental classification permits the reconstruction of five platform stages from the Lower Serdj succession. This classification achieves the principal aims of this paper, especially the vertical facies evolution and is in accordance with standard facies classifications (e.g., Wilson 1975; Tucker and Wright 1990; Flügel 2010).

Results

Facies description and palaeo-environmental interpretations

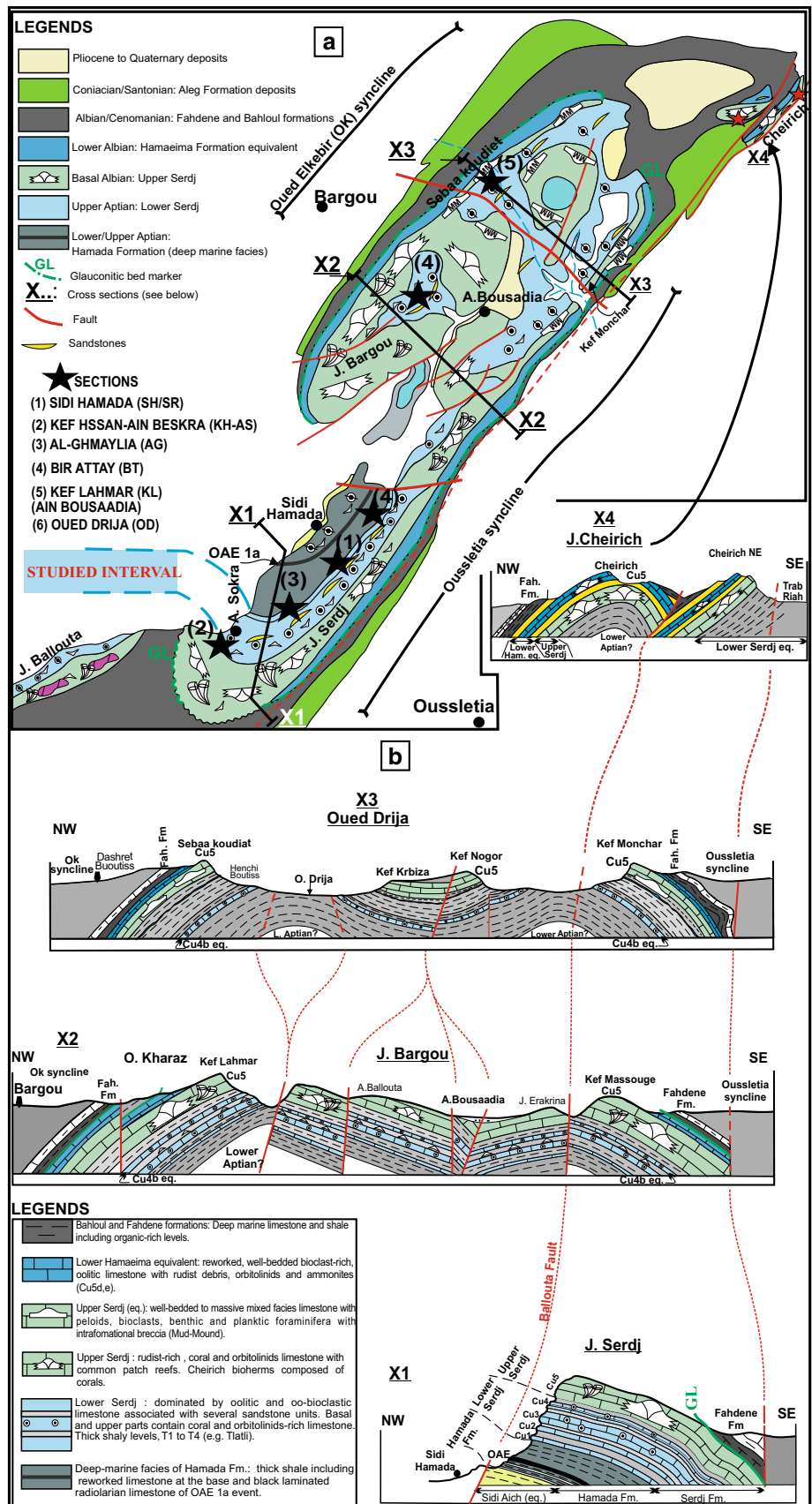
According to previous sedimentological studies (e.g., Tlatli 1980; M'Rabet 1981; Masse 1984; Ouahchi et al. 1998; Troudi 2000; Ben Chaabane et al. 2019; Ben Chaabane 2019), the upper Aptian deposits were formed in broadly shallow-water settings that fostered carbonate productivity. The identified facies, facies zones and stratigraphic levels (Fig. 4 and Table 1) are presented here.

Facies Zone A (FZ A): platform-margin, shoal crest

Facies Zone A characterizes carbonate units Cu3 and Cu4b in sections AG, SH and KH at Jebel Serdj. At sections AG and SH, about 85 m was measured in Cu3 and 25 m in Cu4b. FZ A comprises repetitive shallowing-upward parasequences that begin with green silty shaly units (1–5 m) with several sandstone and/or thin limestone lenses. These pass upward to oolitic and bioclastic limestones (5–17 m thick). Most of the limestone units (Fig. 5a, b) are lenticular with large-scale low-angle (10–15°) cross-stratification, locally bidirectional, suggesting a tidal influence (Fig. 5c).

The FZA contains two facies: (F1) clino-bedded and sigmoidally cross-bedded, well to moderately sorted oolitic packstone to grainstone with combined ripples and small sigmoides (Figs. 5a, b, 6a, b) and (F2) cross-bedded, moderately sorted oolitic to oo-bioclastic pack/grainstone with rare grain aggregates, abundant coral and oyster debris and some orbitolinids (Fig. 6d–f). Furthermore, the bases of some oolitic bodies are wavy and show flaser-bedding (Fig. 7g),

Fig. 3 a Detailed facies map of the Aptian-lower Albian succession of the Serdj-Bargou area which shows the main stratigraphic formations of this period (see Fig. 1) with the main sedimentological features. Note the position of the cross sections (X1, X2, X3 and X4) which are explained below. **b** Schematic structural sections crossing the jebel Serdj-Bargou mega anticlinorium (X1 to X4). Herein, the Aptian-lower Albian stratigraphic succession starts with the Hamada Formation (dark grey) with the OAE 1a event (black area: only cropping out at jebel Serdj), then the grey light blue alternation representing the Lower Serdj deposits; the Upper Serdj or the fifth Serdj carbonate unit Cu5 (green) forms the carapace of the structure. X1 starts near Sidi Hamada village, crosses the Hamada and Serdj formations, and ends by the Fahdene Formation. X2 crosses the jebel Bargou anticlinorium, starts in the Kef Massouge structure (close to Bargou village) and ends with the NW flank represented by Kef Lahmar cliff and Oued Kharraz. The jebel Bousaadia constitutes the heart of the structure which is collapsed by normal faults. X3 lies between Dashret Boutiss village to the NW and Kef Mounchar to the SE. This section crosses the Sebaa Koudiet cliff (south of jebel Touila and jebel Massamet) composed of Cu5 deposits. Note that the heart of the structure is occupied by the Drija Formation (the lateral equivalent of LSF p.p.) comprising the T3, Cu4, and T4 and Cu5 of Kef Krbiza and Kef Nopor. X4 crosses the Cheirich outcrop corresponding to a faulted fold in the prolongation of the Zaghouan reverse fault (modified and completed from Turki 1975, 1985)



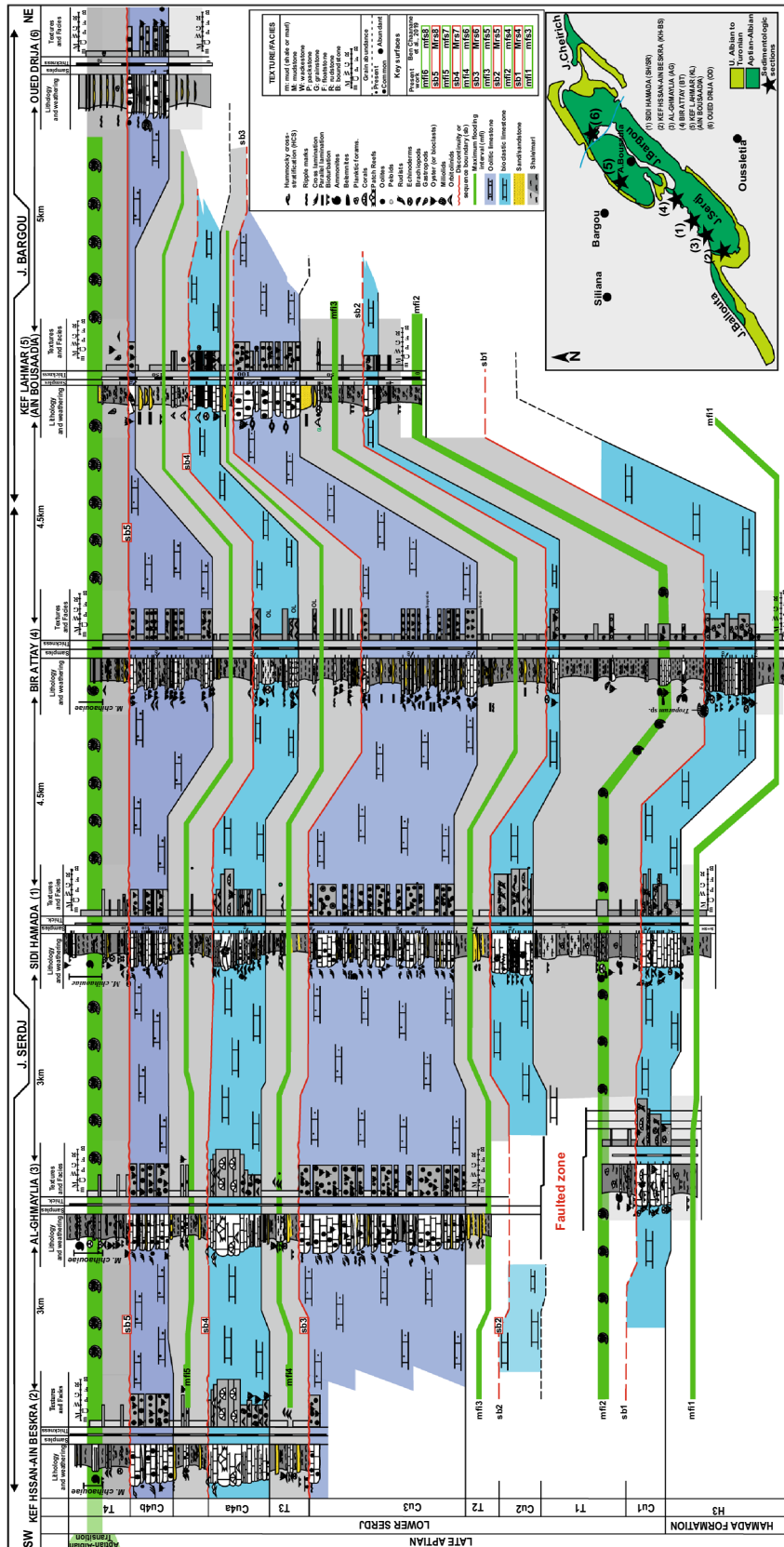


Fig. 4 Lithofacies correlation of the Late Aptian Lower Serdj (LS) platform sections along a proximal (Jebel Serdj)—distal (Drija) transect (SW–NE). Sidi Hamada and Bir Attay sections are the most complete sections that record all the sedimentological events of the LS. For the logs of Alghamaya (AG) and Ain Beskra-Kef Lahsan (AB-KL) are only presented in this correlation as complementary data and additional control points for those of Jebel Serdj. Sequence stratigraphic interpretation based on regional discontinuities of Ben Chaabane et al. 2019 (mrs4-mrs8) labelled in this work sb1 to sb5. The colours distinguish between the terrigenous units (grey), bioclastic limestone (blue) and oolitic-dominated limestone (purple)

Table 1 Facies classification and palaeo-environmental interpretation of the late Aptian deposits (Lower Serdj Formation) of the Serdj-Bargou area

Facies/ Textures/ Thickness		Sedimentary structures/ geometries	Fauna/ Flora	Non-skeletal grains	Description	Depositional Envs./ Interpretations/ Facies zones
F1	packstone to grainstone 0.7-15 m	Large sigmoides and low dip cross-stratification	Oysters, gastropods, echinoderms debris.	Ooids, quartz, mud coated grains	Well-sorted oolitic limestone, lenticular clino-bedded units (10-15° of dip), more than 10 metres of lateral extent, common sedimentary structures with accretional and progradational organization.	FZA PLATFORM MARGIN, SHOAL CREST Tide dominated High energetic setting, above SWB
F2	grainstone/ packstone/ wackestone 3-5 m	Small sigmoides, cross stratification, ripple marks, combined ripples	Debris: echinoderms, rudists, corals, gastropods...	Ooids, mud coated grains, aggregates, quartz	Well to moderately sorted oolitic limestone, metre-thick cross-bedded units separated by silty marl with sandstone beds.	
F3	wackestone/ grainstone 5-8 m	HCS, cross-stratification, groove marks, irregular base	Debris: echinoderms, rudists, gastropods and orbitolinids.	Ooids, aggregates, lithoclasts, peloids, quartz, glauconite	Structure-less oo-bioclastic limestone bodies with irregular bases. Graded grainstone wackestone texture with variable size ooids, moderately sorted. The bodies are decimeter thick with large scale clino-beds, alternating with sandy to silty levels.	FZB UPPER FORE SHOAL Moderately to high energetic setting, sporadically influenced by storm action. These deposits are the result of the progradation (or shedding) of platform edge sediments. Near SWB
F4	grainstone/ packstone/ wackestone 0.5-1.5 m	HCS, cross-stratification, flaser and wavy bedding, ripple marks	Orbitolinids, oyster shells, gastropods and coral debris.	Ooids, peloids, mud coated grains, lithoclasts, quartz	Fine oolitic, moderately to poorly sorted with packstone to grainstone. These limestones are capped by oysters lumachelle or orbitolinid-rich tempestites.	
F5	wackestone/ grainstone 0.2-1.5 m	Small scale lenses, parallel stratification	Orbitolinids, echinoderms, benthic foraminifera	Ooids, lithoclasts, quartz	Silty marls/ shales alternating with orbitolinid-rich and oyster debris limestone, oo-bioclastic limestone and sandstone levels.	FZC DISTAL SHOAL, DISTAL SLOPE Most of the deposits resulting from the sea-level fall and the reworking (by storm waves) of previous deposits of the shoal crest. Below SWB
F6	wackestone/ grainstone 0.1-0.7 m	Cross lamination, ripple marks	Bioclasts, corals and rudists debris, ammonites.	Ooids, peloids, mud coated grains, quartz, aggregates, lithoclasts	Moderately sorted oo-bioclastic tempestites organized in decimeter-thick lenticular levels with the presence of ammonites.	
F7	wackestone 0.2-0.6 m	Tabular beds, common bioturbation	Oysters, debris, echinoderms, rudist debris, annelids, gastropods.	Peloids, mud coated grain, ooids? quartz	Decimetre-thick, well-bedded bioturbated silty limestone with micro-bioclastic peloidal wackestone texture in several levels.	FZD MIDDLE RAMP WITH "PATCH REEFS" above SWB
F8	wackestone/ packstone/ rudstone 0.3-0.7 m	Tabular beds, bioturbation	Orbitolinids, echinoderms, corals and rudist debris, miliolids, textularids, annelids, gastropods, oysters.	Gravel, mud coated grains, ooids	Well-bedded limestone rich in orbitolinids, miliolids, bioclasts and rare corals and rudists debris. some beds composed of rich ooids and orbitolinid facies.	
F9	boundstone/ rudstone/ floatstone 5-15 m	Massive to sub-massive biostromes.	Corals, sponges, rudists, orbitolinids, oyster debris...	Peloids, ooids, gravel, quartz	Coralline boundstone forming biostromes, with orbitolinids and other organisms.	FZE
F10	wackestone 10-12 m	Bioturbation	Oysters, echinoderms, brachiopods, annelids, ammonites, planktic and benthic forams	Peloids, lithoclasts	Decimetre-thick, rich bioclastic, nodular bioturbated grey well bedded limestone.	FZF OUTER RAMP Wave influence Near to or below SWB
F11	wackestone/ packstone 15-30 m	Bioturbation	Orbitolinids, echinoderms, oysters, brachiopods, ostracods, planktic forams	Glauconite	Alternation of very bioturbated orbitolinid bearing green silty marl with well-bedded limestone rich in orbitolinids, benthic foraminifera, ostracods, shark's teeth and common thick oysters.	
F12	sandstone/ limy sandstone	Parallel lamination, HCS, ripple marks, groove marks	Bioclasts	Quartz, ooids, peloids, lithoclasts	Alternation of silty marls and decimetre – thick sandstone with sedimentary structures	FZG OFF PLATFORM TO BASIN below SWB
F13	mudstone/ shale/ marls	Bioturbation	Planktic and benthic forams, ammonites, echinoderms, brachiopods, oysters, trigonids	Quartz, glauconite	Alternation of rich planktic, benthic foraminifera shale/ marl and nodular fine to muddy limestone containing ammonites.	

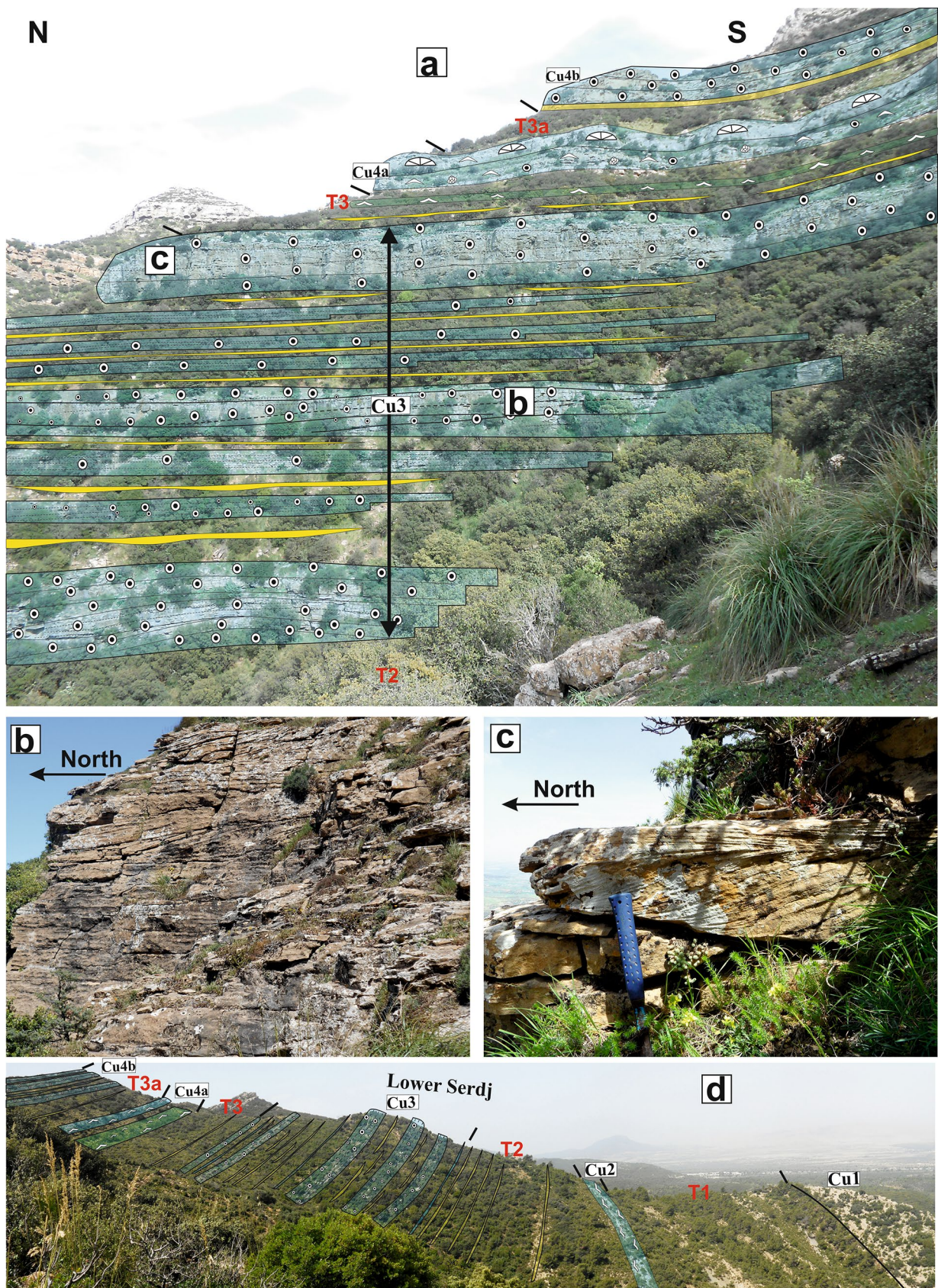


Fig. 5 **a** Photo-interpretation of the Lower Serdj, Sidi Hamada section, shows the main lithofacies encountered and an overview of their composition. The Cu3 shows metre-thick oolitic bodies overlain by the terrigenous unit T3 which itself is overlain by the fourth carbonate unit Cu4 (**a**, **b**). **b** Internal organization of the ooid-rich units of the Cu3 in the SH section showing tide-dominated cross-stratification with clear northward transport. **c** Small-scale tide-dominated cross-stratification with northward migration of oolitic facies, Cu3, SH section. **d** Photo-interpretation of the Lower Serdj units, Bir Attay section, that exhibits an important facies and thickness variations when compared to the same section at the Sidi Hamada section. These lateral variations have been observed in Cu2 and Cu4a units

associated with calcareous sandstone. The tops of the bodies are marked by fossiliferous units encrusted by thick oysters and with ripple marks (Fig. 7e). The typical ooids that compose this shoal bank, especially in unit Cu3, are well sorted with quartz grain nuclei (Fig. 6). The facies of this zone, with their sedimentary structures, clearly reflect an active and relatively continuous, tide-dominated high-energy setting for units Cu3 and Cu4b (Fig. 7a–d).

Facies Zone B (FZ B): upper-fore shoal

The facies of this Zone (FZ B) have been mostly defined from the BT to KL-BS transect. Herein, the Cu3 and Cu4b units show significant lateral variations compared to the southern part of jebel Serdj. The oolitic bodies become separated by thicker shaly units (7–15 m thick) where their thicknesses are thinner than the SH section (5–10 m). They show a wide low-dip clino-bedded geometry, especially for those of Cu3 (Fig. 5d).

The facies of this zone have been recognized within several oolitic limestone bodies of Cu3 and Cu4b units. It is composed of two facies: (F3) and (F4). The F3 facies consists of oolitic limestones (1–2 m) which are fine to medium oolitic well sorted and locally graded grainstone/packstone (Fig. 8a, b). These limestones are capped by oyster or orbitolinid-rich tempestites (Fig. 7c). The ooids are radial and concentric with a quartz or shell nucleus. Cross stratification (10–15° of dip), low-angle clinoforms and parallel bedding are present in this facies zone (Figs. 7c, 8b). The F4 facies consists of structure-less bioturbated oo-bioclastic units (1–5 m thick) composed of moderately sorted graded packstone to grainstone with irregular bioclastic basal parts, especially at the BT section. Different sizes of ooids occur, along with coated grains, common quartz grains and aggregates (Fig. 8c, d). Groove marks, low-angle bedding, hummocky cross-stratification and lithoclasts are common and

indicate northward transport by tidal and storm currents (Fig. 7f, h). The transported calcareous grains are derived from the platform crest and then moved towards deeper water settings. These grains are mixed with shallow-marine platform skeletal grains (Fig. 8b, c), such as orbitolinids and oyster debris.

Facies zone C (FZ C): distal shoal or distal slope

This facies zone (FZ C) corresponds to the lower part of the Cu3 deposits at KL-BS, and the Cu4b unit deposits at the Drija section. Two facies represent this zone. The first (F5) consists of lenticular oo-bioclastic limestone, arranged in thin flat sheets (1–2 m thick) within marly units. They are coarse-grained proximal storm deposits, with poorly sorted broken ooids, benthic foraminifers, mud-coated grains, aggregates, lithoclasts, orbitolinids and other bioclasts (Fig. 9). This facies forms the lower 2 m of Cu3 at the KL section.

The second Facies F6 of this Zone consists of an alternation of decimetric oo-bioclastic limestone (0.2–0.7 m thick) and tempestites. They are rich in oyster debris, lithoclasts, orbitolinids, bioclasts and common ammonites. Centimetre to decimetre beds (0.1–0.3 m) of sandstone, silty marl and shale also occur in this facies (Fig. 9a, b). Most of the thin beds and sandstones are lenticular with limited lateral extent (Fig. 9b); marls are rich in planktic foraminifers (Sedjil 1981).

Most of the grains and tempestite accumulations of FZ C were derived from the inner parts of the shoal complex. They were re-deposited by storm events within deeper water settings (Fig. 9a, b) and depressions as suggested by the presence of lithoclasts, planktic foraminifers and ammonites (Fig. 9b) within the background micrite-shale (Sedjil 1981) during the deposition of Cu4b at Oued Drija. The bioclastic tempestites contain common glauconite grains.

Facies Zones D and F (FZ D and FZ E): middle ramp with "patch reefs"

This facies zone was identified for the Cu1, Cu2 and Cu4a unit limestones of jebel Serdj (SH, KH-BS and AG sections). They are characterized by grey to brownish decimetre to metre-thick limestones dominated by corals, oysters, rudists (debris), sponges and orbitolinids with common miliolids and echinoderm debris (Figs. 10, 11).

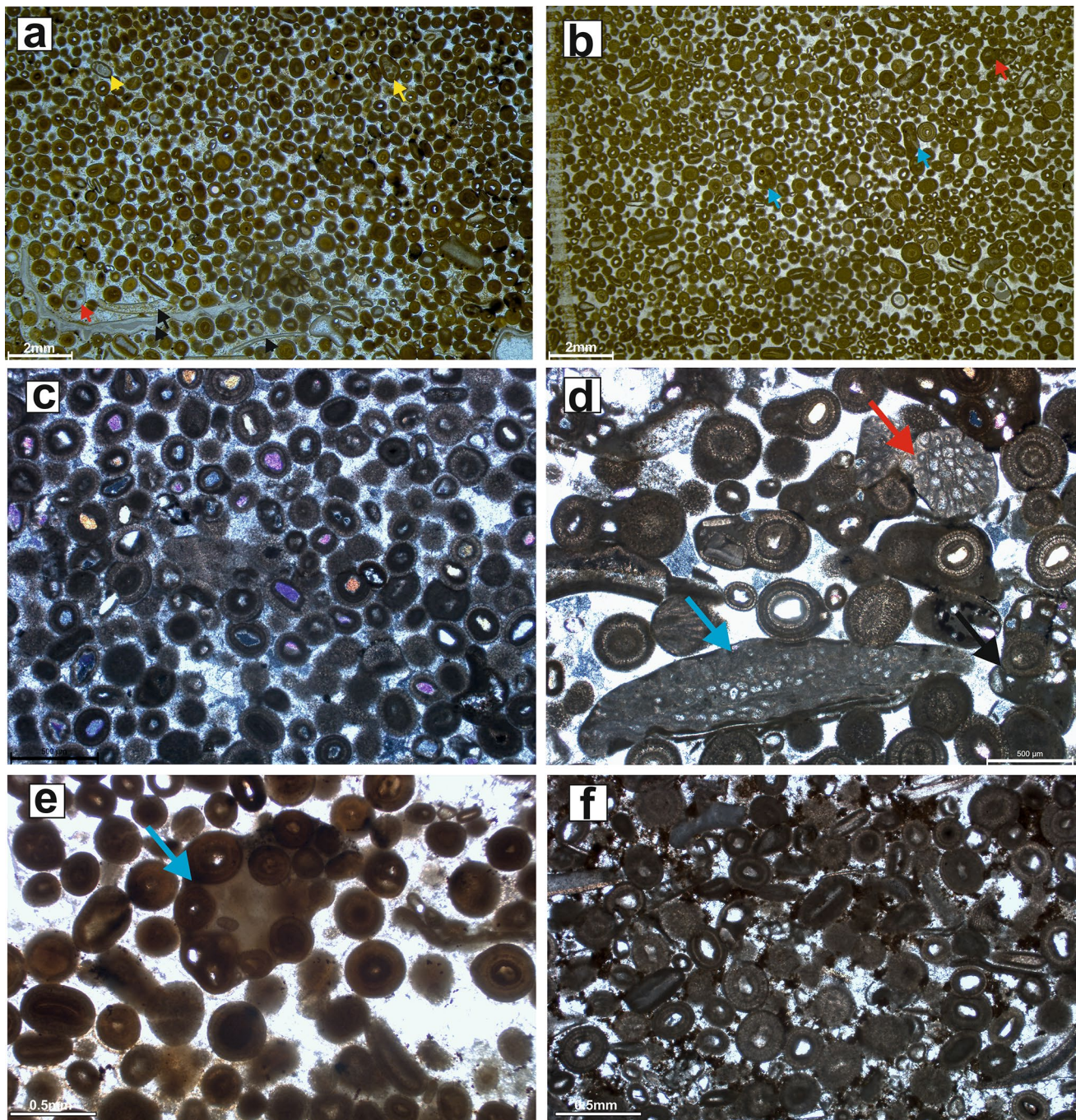


Fig. 6 Photomicrographs showing the main microfacies of the FZA. **a** well-sorted oolitic grainstone with some bioclasts, SH section, Cu3, sample Sh 43. **b** Well-sorted medium to fine oolitic grainstone. Note the presence of small aggregates and ooids with thinly laminated fine-concentric cortices, SH section, Cu3, sample Sh 56. **c** Moderately sorted oolitic grainstone where most ooids have quartz nucleus, SH section, Cu3, Sh 60. **d** Oolitic-skeletal grainstone with orbitolinids

(blue arrow), coral debris (red arrow) and some composite grains (black arrow), SH section Cu3, Sh 48. **e** Sparsely oolitic cemented grainstone with concentric cortices. The aggregate grain (blue arrow) could be reworked, SH section, Cu3, sample Sh 43. **f**: Moderately sorted oolitic grainstone with common coated-grains and broken ooids, SH section, Cu3, Sh 55

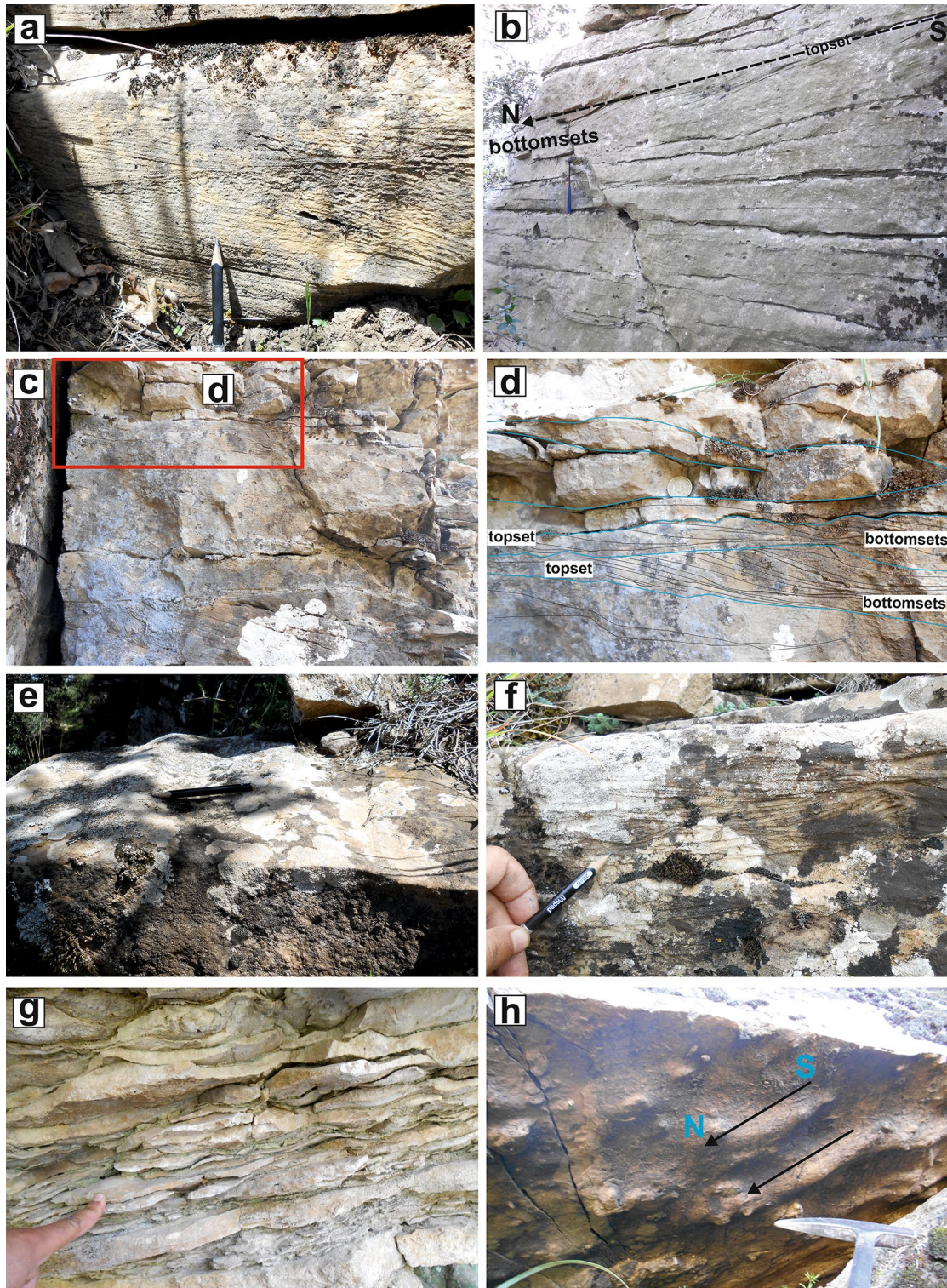


Fig. 7 Examples of sedimentary structures associated with the oolitic facies for the sedimentary units Cu3 and Cu4b. **a** Oolitic grainstone with cross-stratification (FZ A), Cu3, SH section. **b** Metre-scale low-angle clino-bedded oolitic limestone beds (FZA), Cu3, SH section. The interrupted line shows the horizontal topsets (southern side) whereas the bottom-sets are located to the north, clearly showing the northward migration. **c** Oolitic limestone (F3) with clinoforms. **d** Detail of **c** showing two small-scale (muscle shape) cross-bedded oolitic limestones and

each overlain by irregular wavy bedding. **e** Ripple marks common in the upper part of Cu3, SH section. **f** Hummocky cross-stratification (FZ B) within the oolitic facies of Cu3 unit, BT section. **g** Flaser-wavy bedding associated with sandy oo-bioclasic facies in the lower part of one of the oolitic bodies of Cu3, SH section. These kinds of structures are generally located in the transgressive part of the shallowing–shoaling upward parasequences. **h** Groove marks at the base of an oolitic bed of Cu4b (at SH) showing northward transport

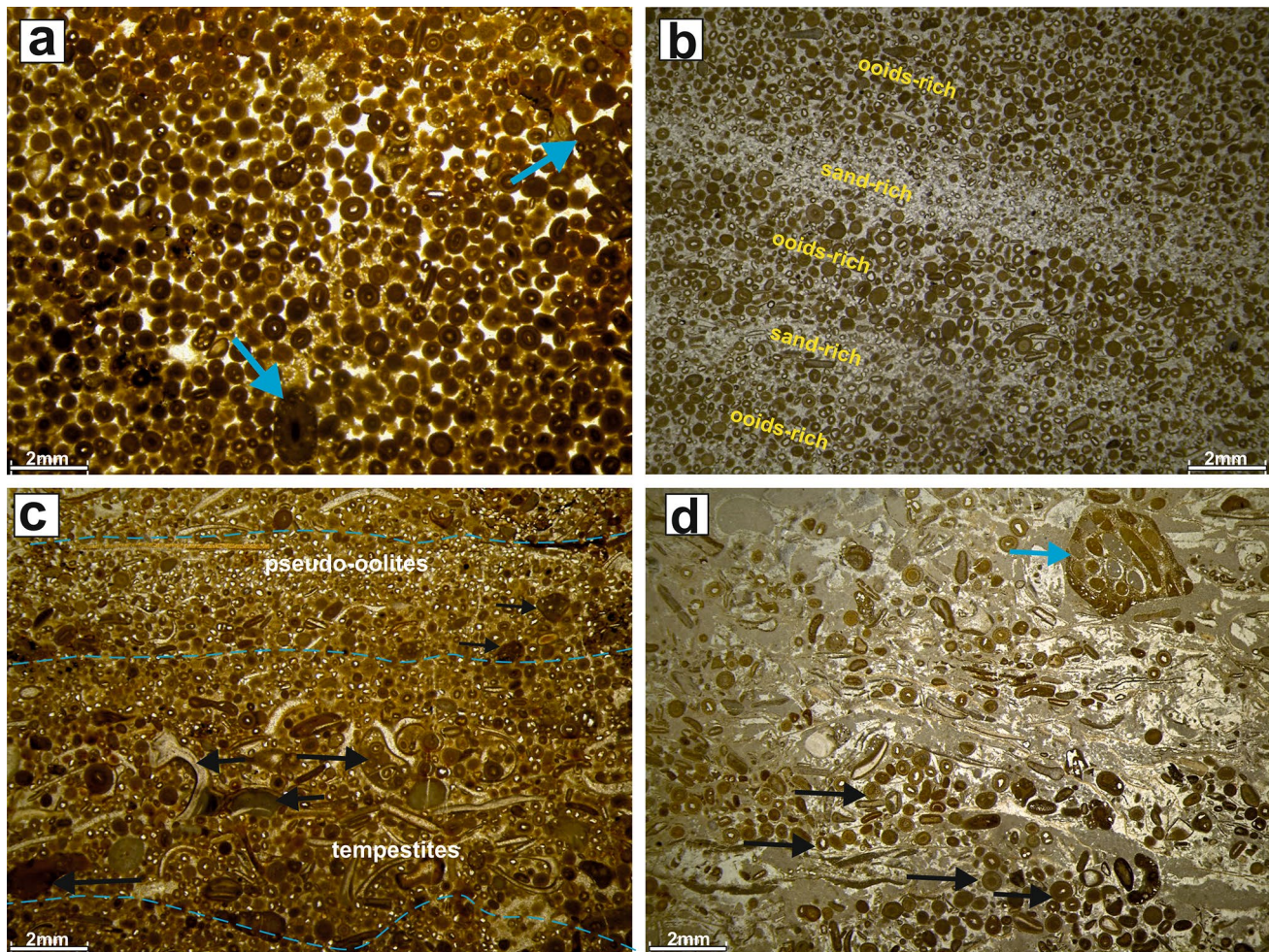


Fig. 8 Photomicrographs showing the main microfacies of the FZ B. **a** Well-sorted oolitic grainstone. Most ooids have a similar size; rare extraclasts (blue arrow), BT section, Cu3, BT 81. **b** Oblique graded oolitic-dominated facies (10–15° dipping to the north). Note the alternation between rich oolite laminae (bioclasts and coated grains also present) and quartz-rich laminae with common pseudo-oolites, SH section, Cu3, Sh 57. **c** Poorly sorted normally graded oo-bioclasic

grainstone, consisting of an alternation of ooid (or pseudo-ooid)-rich and bioclast-rich laminae, with common lithoclasts (black arrow) and oolite tempestites (laminae separated by dashed line), BT section, Cu3, BT 28. **d** Poorly sorted oo-bioclasic grainstone with thinly laminated radial cortices (black arrow), compound ooids and lithoclasts made of bioclasts and serpulids (blue arrow), BT section, Cu3, BT 41

Three facies (F7 and F8) have been identified for this zone: (F7) consists of decimetre-thick, well-bedded bioturbated silty micro-bioclasic peloidal wackestone (Fig. 10a, b). This facies was observed for the Cu1 (2 m at AG; 12 m at SH; 17 m at BT) and thinner in Cu2 (2 m at SH) and Cu4a (3 m at KH-BS; 2 m at AG) units. The scarcity of fossils could indicate a low biological diversity or short transport, due to periodic storm wave action, of the sediment (Fig. 10a, b) from proximal settings (south of jebel Serdj).

The FZ E represented by the facies F8 consists of well-bedded limestones rich in orbitolinids, miliolids, bioclasts,

rare corals, rudist debris, pseudo-oolites and gastropods (Figs. 10b, 12e, f). This facies characterizes the Cu1 (2–4 m at KH-BS and AG), Cu2 (middle part, 2 m at SH; Fig. 11) and the Cu4a (2–4 m at KH-BS and AG sections) units. It is observed below some massive limestone bodies (Fig. 10c) or as their lateral, basinward equivalents.

The F9 facies is composed of massive to sub-massive limestone extending laterally for more than 20 m as a "biostrome" (Figs. 10c, 11) rich in coral (Fig. 12a–d) associated with sponges, rudist debris and orbitolinids. This facies characterizes the Cu2 (two bodies: 5–8 m at AG and SH

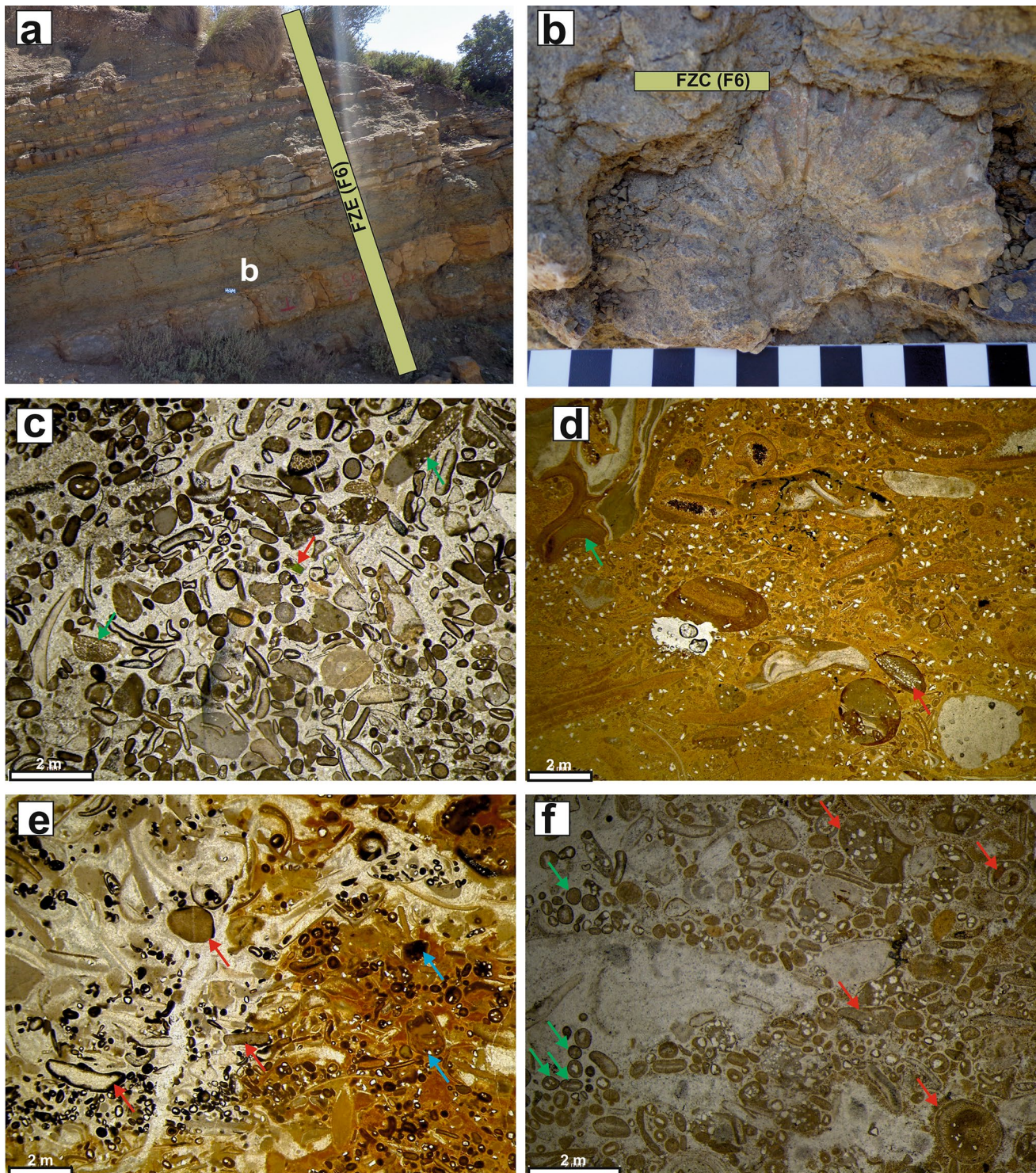


Fig. 9 Photomicrographs showing the main microfacies of the FZ C. **a** Alternation of oo-bioclastic cm to dm-thick beds with silty marl. Note that the oo-bioclastic limestones contain ammonites (**b**), the Cu4b equivalent at the OD section. **c** Moderately sorted grainstone with sparse mud-coated grains (cortoids). Herein, most of the skeletal grains have micrite envelopes and the inter-granular space is occupied by calcite cement. The coated grains consist of echinoderm plates, orbitolinids (green arrow), aggregates and other bioclasts. These facies reflect a relatively moderate energy environment, especially with the occurrence of glauconitic (red arrow). KL-BS section, Cu3, KL-BS 6. **d** Very poorly sorted sandy oo-bioclastic grain-

stone with common lithoclasts and coated coarse grains within fine terrigenous sediment. Most of the ooids have a quartz nucleus and associated grains consist of serpulid debris (green arrow), orbitolinids (red arrow) and aggregates/extraclasts. KL section, Cu3, KL-BS 13. **e** Sparsely oo-bioclastic grainstone/tempestite with common cortoids and mud-coated grains (red arrow) and aggregates (blue arrow). OD section, Cu4b, OD 2. **f** Oo-bioclastic tempestite with grainstone texture. Common bioclasts/lithoclasts, gastropods (red arrow) and aggregates (blue arrow). Note that some ooids have a fine mud cortex (green arrow). OD section, Cu4b, OD 3

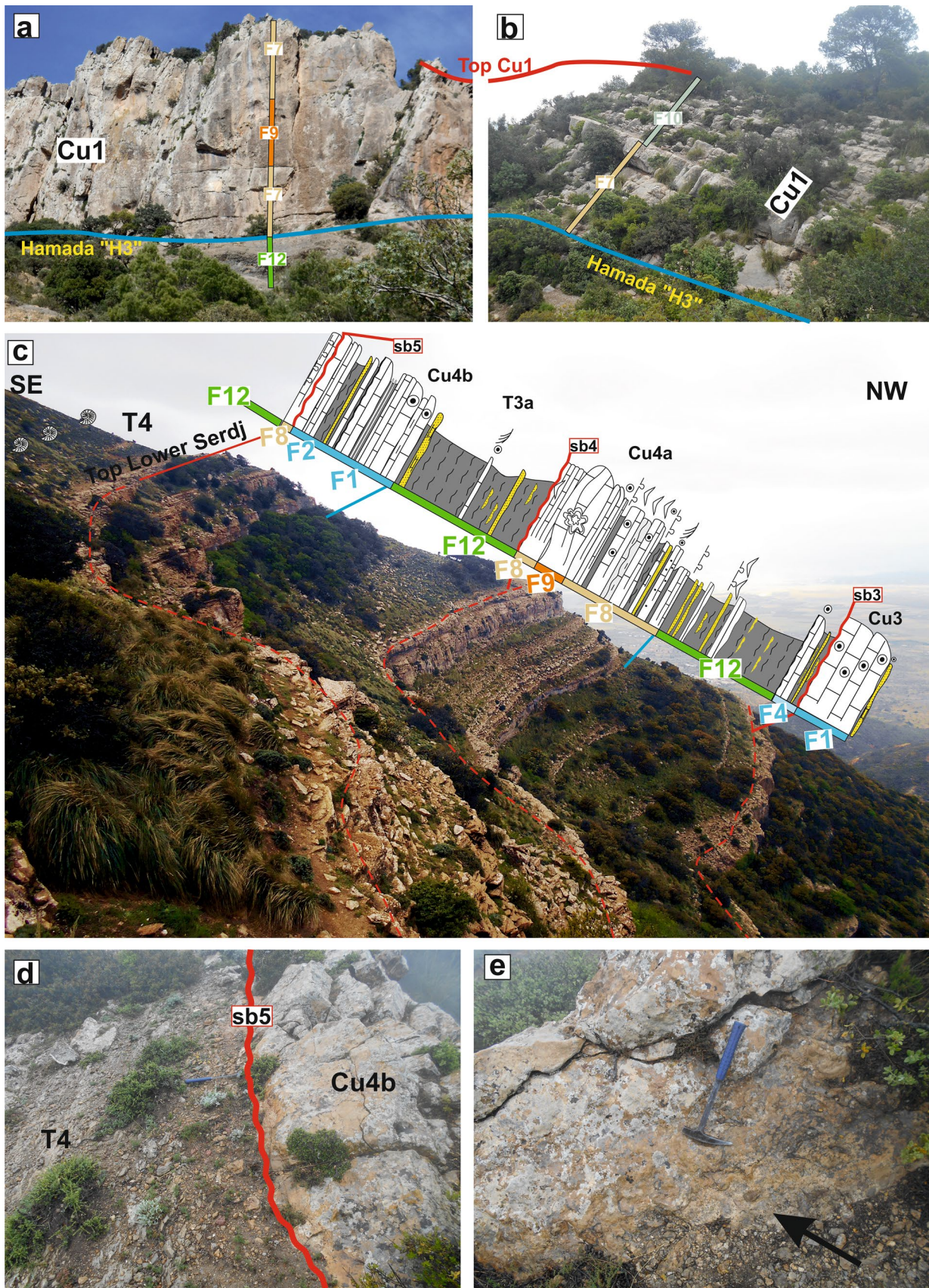


Fig. 10 a,b Overview of the first unit (Cu1) that shows lateral facies changes from SH, where it is composed of well-bedded to sub-massive limestone then passing in the BT section to an alternation, especially at the upper part, of well-bedded limestone and nodular limestone. **c** Panoramic view of the upper part of the Lower Serdj (Cu3, T3 and the sub-units a, b of Cu4) of the SH section with the corresponding detailed logs and facies interpretation (F). The Cu3 unit and the second (Cu4b) are represented by oolitic to oo-bioclastic deposits that developed within a shoaled platform system. The Cu4a unit is dominated by coral-rich biostromes and orbitolinid-rich limestones deposited within a homoclinal ramp system (see below for the detailed environment interpretation). Note that the two sub-units of Cu4 are separated by alternating marl and sandstone of T3a (according to Ben Chaabane 2019). **d** Top-surface (Sb5) of the oolitic deposits of the Cu4b unit overlain by planktic foraminifera-rich marl of the T4 unit. **e** Detail of Sb5 boundary showing sub-exposure ferruginous surface (arrow)

sections), Cu4a (5–15 m at KH-BS, AG and SH sections), and locally for Cu1 (about 1 m at SH) of Jebel Serdj.

Facies Zone E (FZ E): outer ramp

Facies F10 characterizes the upper part of the Cu1 unit (12 m thick) at the BT section and Cu 2 both at BT and KL-BS

sections (Fig. 13). The upper Cu1 unit at BT is mainly composed of bioclastic, nodular, highly bioturbated grey limestones (Fig. 13a, b). The dominant grains are essentially oysters and echinoderms, serpulids associated with belemnites, brachiopods and many large (> 20 cm diameter) ammonites (Fig. 13b). The corresponding microfacies show bioturbated wackestone (micrite and clay) with bioclasts and serpulid debris and common planktic foraminifers (Fig. 14c–f).

The second facies F11 consists of an alternation of very bioturbated orbitolinid-bearing green slightly silty marl (Fig. 13b, c) with orbitolinid-rich well-bedded limestone (12–22 m; unit Cu4a, at BT and KL-BS sections). The marl, which commonly contains calcareous nodules, is bioturbated, containing orbitolinids, thick oysters, echinoderms, ostracods and common planktic and benthic foraminifera (Fig. 13b, c).

Facies Zone F (FZ G): off-platform-basin setting

This facies zone characterizes several stratigraphic levels of the Lower Serdj, especially those with terrigenous units (T1 to T4). Two elementary facies were identified for this zone. The first facies F12 is represented by an alternation of

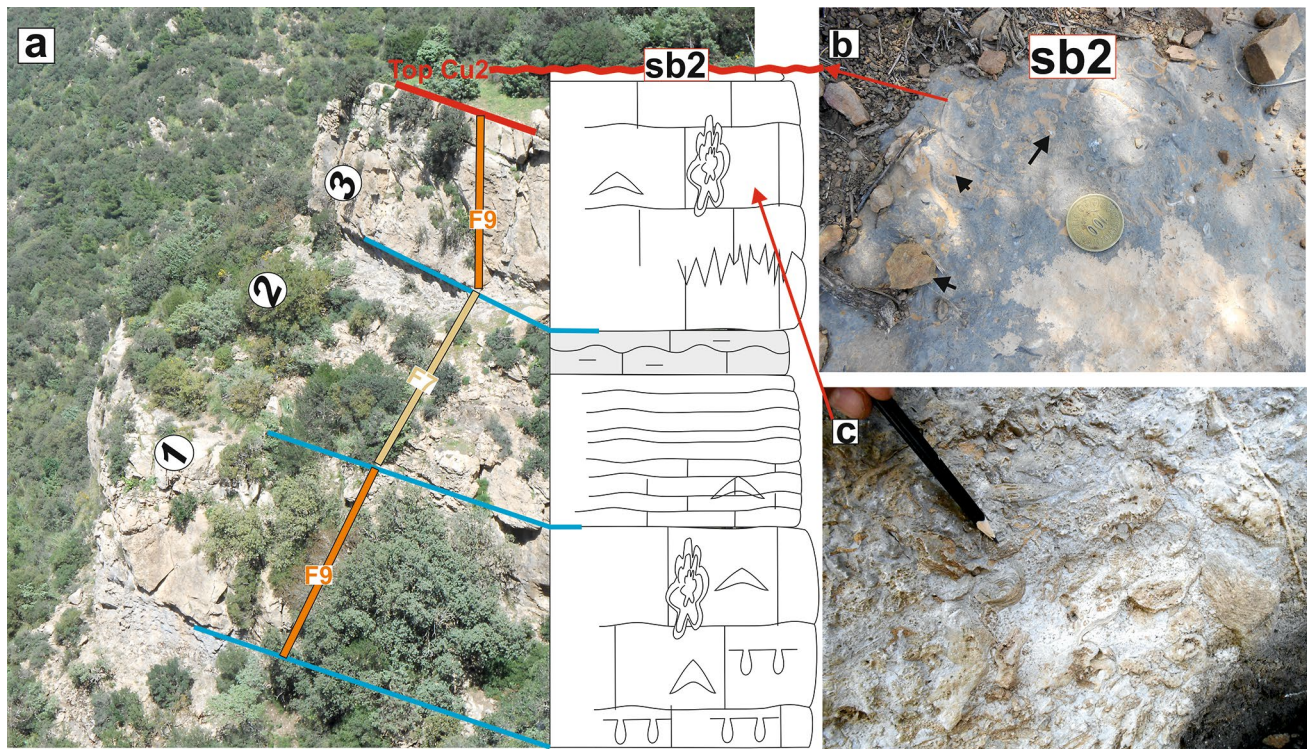


Fig. 11 a Overview of the second unit at the SH section composed of two (1 and 2) sub-massive sub-units. **b** Top surface of Cu2 encrusted by oyster shells with small cavities filled by ochre silt (arrows) from

subaerial exposure at the sb2 sequence boundary. **c** Coral-rich rudstone associated with other bioclasts

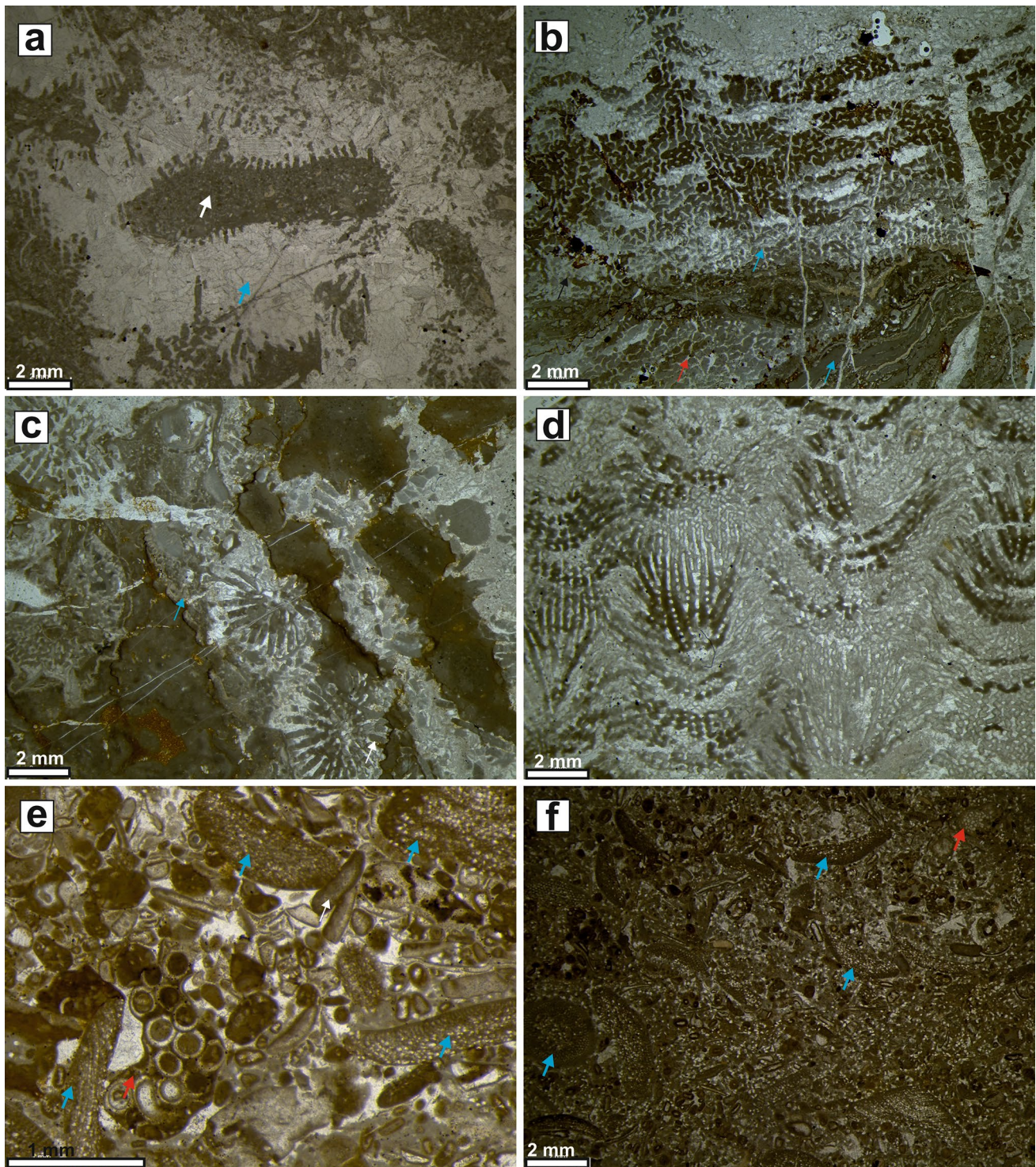


Fig. 12 Photomicrographs showing the main microfacies of the FZ D. **a** Encrusting coralline algae (blue arrow) in boundstone. The coralline algae trapped fine peloidal (white arrow) silt. SH section, Cu1, Sh 4. **b** Dominant coral bindstone/boundstone associated with *Bacinella-Lithocodium*? SH section, Cu2, Sh 27. **c** Coral framestone facies displaying fine bioturbated muddy matrix between the coral tabulae reflecting a quiet to moderately energy, SH section, Cu2, Sh

29. **d** Stromatoporoid boundstone with common fine trapped sediment, SH section, Cu2, Sh 23. **e** Orbitolinid-rich, serpulid, bioclastic, mud-coated grain packstone (F11), SH section, Cu4a, Sh 89. **f** Slightly sandy orbitolinid-rich (blue arrow) grainstone with peloids, mud-coated grains, ooids (?), coral debris (red arrow) and common bioclasts (F11), SH section, Cu4a, Sh 91. (Scale bar: 2 mm)

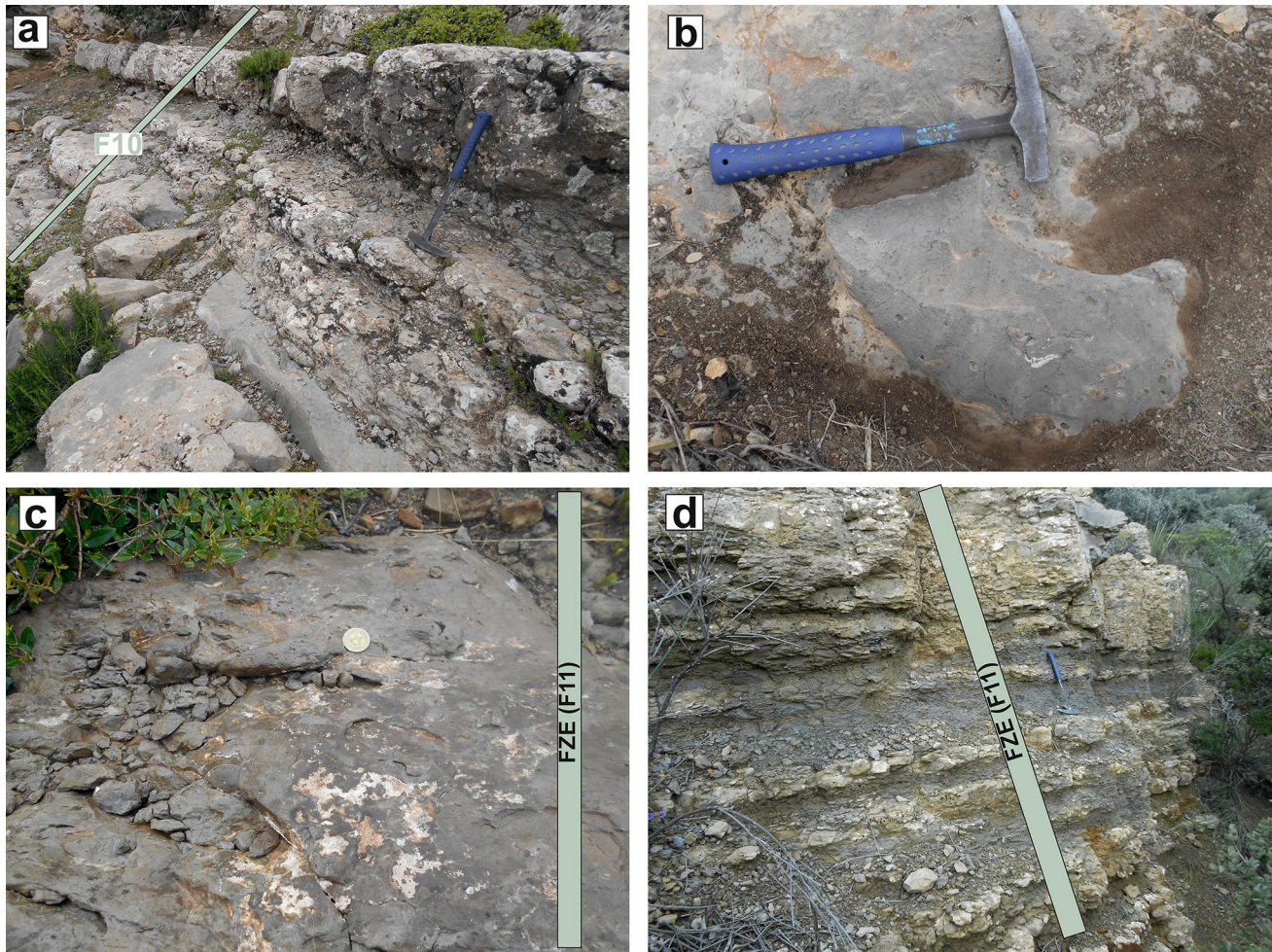


Fig. 13 **a** and **b** detail (F10) of unit Cu1 at the BT section showing an alternation of oyster-rich bioturbated nodular limestone and fine bioclastic limestone with ammonite at top (**d**). **c** Orbitolinid-rich limestone, the lateral equivalent of unit Cu4a at the BT section (F11). **d**

An alternation of indurated orbitolinid-rich and echinoderm marl and silty-sandy orbitolinid marl with rare thick oysters and echinoderms, unit Cu4a equivalent at the KL section, jebel Bargou (F11). These facies represent the distal part of a homoclinal ramp, FZ E

silty grey marl containing ostracods, benthic foraminifera and rare planktic foraminifera (according to Tlatli 1980; Heldt et al. 2010) and several interbedded sandstones (Fig. 15a–d) and calcareous sandstone beds (Fig. 15d–f), occurring especially within terrigenous units T2, T3 and T3a (Fig. 15). The sandstones consist of massive fine sandstone (0.7–1.2 m thick) and laminated fine to medium sandstone (Fig. 15a–d) which are probably lateral equivalents

to some northern carbonate units. The second one F13 is dominated by shaly and marly deposits rich in planktic and benthic foraminifera alternating with bioclastic and orbitolinid-rich nodular limestone, with many ammonites locally (*Acanthohoplites*, '*Hypacanthoplites*' sp., *Mellegueiceras chihouiae*). These units include several nodular and bioclastic limestones. Facies F13 occurs within the T1, T3 and T4 terrigenous units.

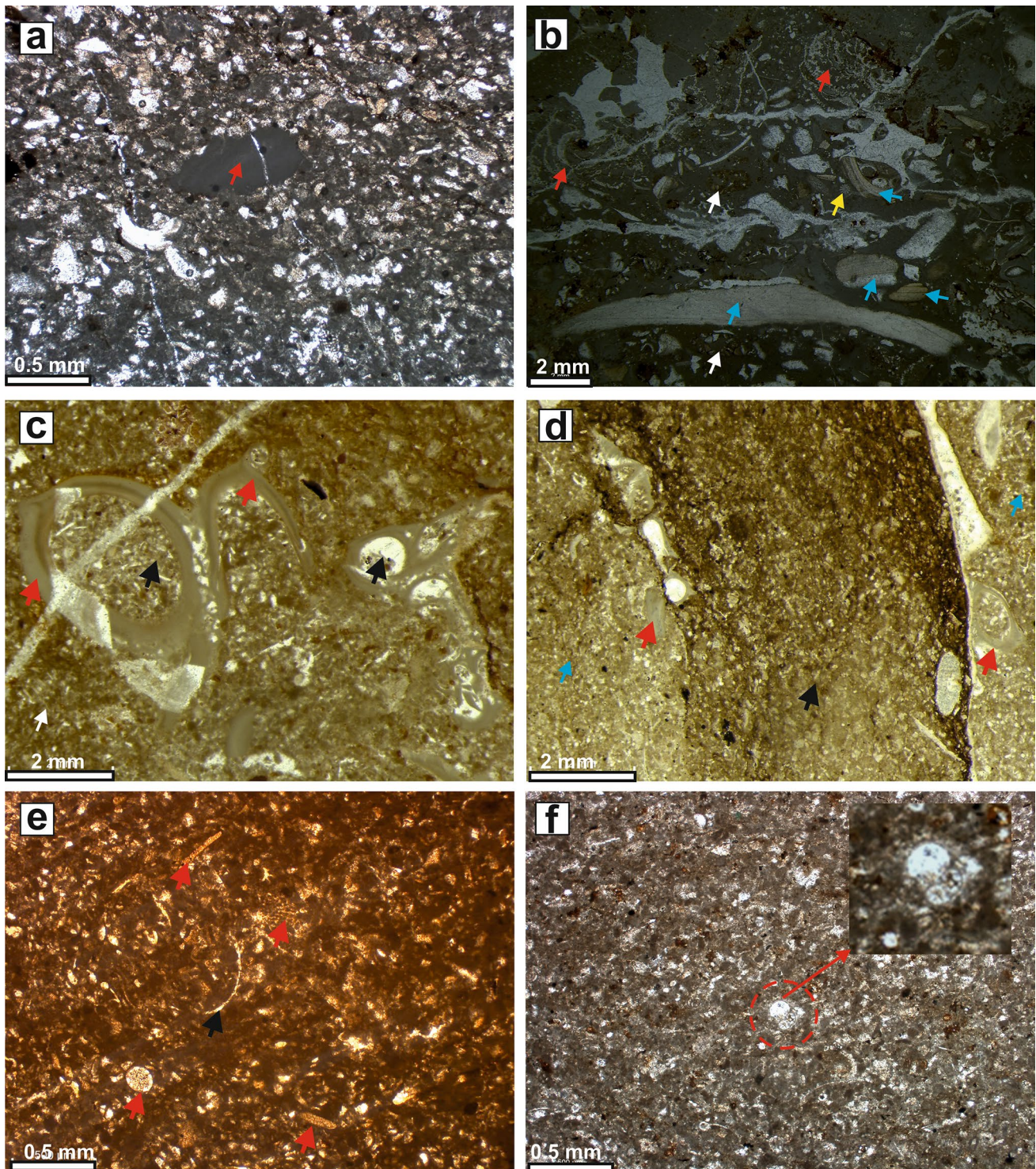


Fig. 14 Photomicrographs of the main facies of FZ D and FZ F. **a** Peloid-rich micro-bioclastic pack-grainstone (F7) with common echinoderm and oyster debris and some lithoclasts (arrow), SH section, unit Cu1, Sh 3. **b** Sparse coarse-grained rudstone with bioturbated matrix (F7). Common bioclastic debris includes rudists (blue arrow), echinoderms, sponges (red arrow) and aggregates (white arrow), SH section, unit Cu2, Sh 37. **c** Scattered and broken serpulid tubes (red arrows) within a peloidal facies (white arrow). Serpulid sections cemented by calcite or filled by different sediment (black arrows)

than host matrix. BT section, the upper part of unit Cu1, BT 21. **d** Burrowed peloidal bioclastic wackestone (blue arrow) with common serpulid debris (red arrow). Note different sediment filling the burrow (black arrow) and outside the burrow, top of the lower part of unit Cu1, BT section, BT 21. **e** Bioclastic peloidal wackestone with common oyster (black arrows) and echinoderm (red arrow) debris, unit Cu1, BT section, BT 25. **f** Microbioclastic facies with common peloids and planktic foraminifera. unit Cu2, BT section, BT 27

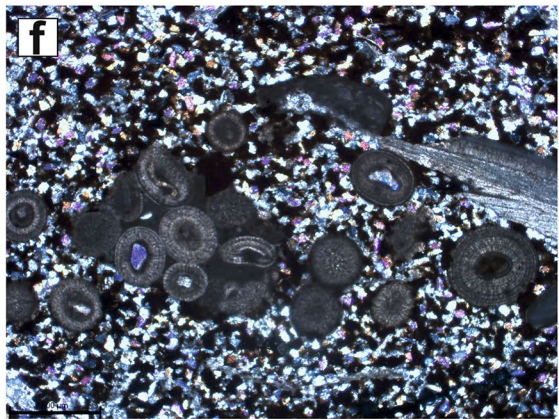
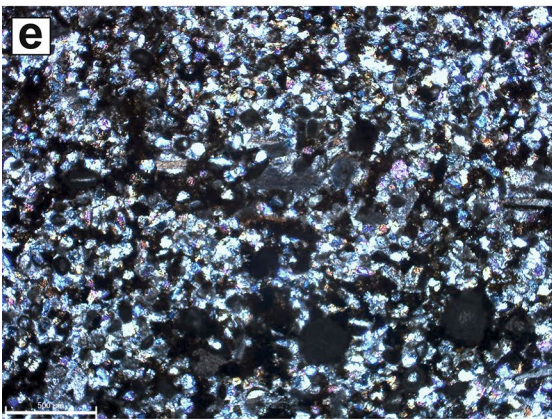
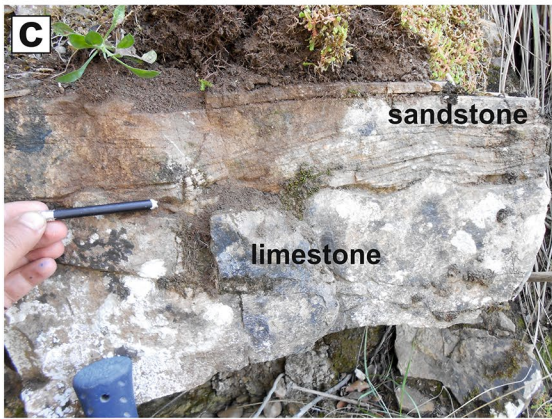


Fig. 15 Field photographs of the main facies in the FZ G. **a** Bioturbated fine to medium sandstone with planar lamination, F12, T2, KL-BS section. **b** Cm to dm-thick fine sandstone beds with silty marl interbeds, F12, T3a, SH section. **c** Oolitic limestone with ripple marks at the top, overlain by fine sandstone with HCS, F12, T2, BT section. **d** Dm-thick laminated calcareous sandstone bed within silty marl and basal groove marks, F12, T3a, BT section. **e** Calcareous peloidal sandstone, F12, SH section, Cu3, Sh 60. **f** Sandy limestone with common ooids and bioclasts, F12, SH section, unit Cu4b, Sh 114. **g** Thick planktic foraminiferal shales of unit T1 (F13), BT section. **h** Fine bioclastic ammonite-rich ochreous limestone (F13) within shale of unit T1, SH section

Depositional models and carbonate platform evolution

Carbonate platforms have distinctive and unique features that respond to the geotectonic context and physical, chemical and biological conditions of that specific interval of Phanerozoic time (Pomar and Hallock 2008). Herein, the carbonate units of the LSF display distinct depositional profiles (Figs. 16, 17), facies-zone distributions and platform architecture through the Late Aptian.

Stage 1, Cu1 carbonate unit

In response to the pronounced marine regression after the deep-water shaly Hamada Formation, the sedimentary record of the platform was marked by the installation of the overlying Cu1 unit carbonates exposed at jebel Serdj (Figs. 2, 4). The Cu1 facies were deposited on a homoclinal ramp (middle to outer parts) that developed before the time of the sequence boundary sb1 (Mrs4 of Ben Chaabane et al. 2019) and they constitute the first prograding stage of the LSF platform (Figs. 4, 16a).

At the SH and AG sections and in the southern part of jebel Serdj, the deposits of Cu1 consist of well-bedded limestones (25–27 m thick) dominated by a microbioclastic peloidal texture and including some small coral biostromes. Moreover, the existence of common rudist debris (Fig. 10a) suggests that an inner ramp system was present south of jebel Serdj (Central Atlas of Tunisia; M'rabet 1981). Furthermore, the shallow-water biota, associated with relict mud-coated grains for the two facies F7 and F8 within a muddy matrix, confirm a low to moderate energy setting for Cu1 at the SH and AG sections.

The counterpart of the Cu1 at the BT section includes in its lower part, well-bedded limestone (18 m thick), similar to that in the SH section (Fig. 10a, b). However, the upper part (8 m thick) consists of nodular limestone (Fig. 13a, b) with echinoderms, serpulids, oysters, rare benthic and planktic foraminifera and ammonites with a mudstone to wackestone texture (Fig. 14c, d). They indicate a more proximal setting

than that described at the SH and AG sections and show a deeper water palaeo-environment on a clear outer homoclinal ramp. Here sedimentation was likely influenced by storm activity that led to sediment reworking (Figs. 14b–d, 16a, 17a).

Stage 2, Cu2 carbonate unit

This stage took place after the transgressive unit T1. It corresponds to a retrograding carbonate platform, before the sequence boundary sb2 (Ben Chaabane et al. 2019; Ben Chaabane 2019; Figs. 4, 16b). The Cu2 carbonates (27 m thick at SH) show the proliferation of shallow-marine biota (Fig. 12) including in situ corals, orbitolinids and common sponges associated with oysters and rudist debris (F8 and F9). Well-preserved coral biostromes dominate the third facies F9 with common sponge and rudist debris. Some coral buildups (Figs. 11, 12) appear to have developed upon local topographic highs, where suitable ecological conditions existed. The dominant organisms suggest mesotrophic conditions and these contributed to the establishment of a homoclinal carbonate platform (Figs. 16b, 17b). The corals and coral-sponge-rudist-orbitolinid facies associated with micrite were developed in a moderate to low-energy setting, near or below fair-weather base, with occasional storm influence (e.g., Ross and Skelton 1993).

Consequently, the dominant-coral facies with biostromes in this stage at the SH section (27 m thick) suggests a middle homoclinal ramp setting with common “patch reefs” (FZE) at jebel Serdj (Fig. 17b). Furthermore, the lithofacies correlation (Figs. 5, 16) shows a significant northward thickness decrease reflected in the absence of coral biostromes at the BT (9 m) and KL (6 m) sections (Fig. 16b). The northward equivalents, at the BT and KL-BS sections, correspond to bioclastic-rich and peloidal wackestone with common orbitolinids, lithoclasts, benthic and rare planktic foraminifera (F11). These grains and textures suggest an outer homoclinal ramp setting (FZ F).

Stage 3, Cu3 carbonate unit

From the sb2 of Cu2 stage, a pronounced change occurred in LSF sedimentation, with a high terrigenous input (Fig. 4; since T2). The Cu3 carbonates were deposited after the transgressive unit T2, including the mfi3 (mfs5 of Ben Chaabane et al. 2019), and capped by the sequence boundary sb3 (Mrs6 of Ben Chaabane et al. 2019). The lithofacies correlation demonstrates that from the southwest to the northeast (Figs. 1b, 3, 16c), there is a net thickness decrease and facies change, suggesting that deposition took place in a shoaled ramp setting (Fig. 17c).

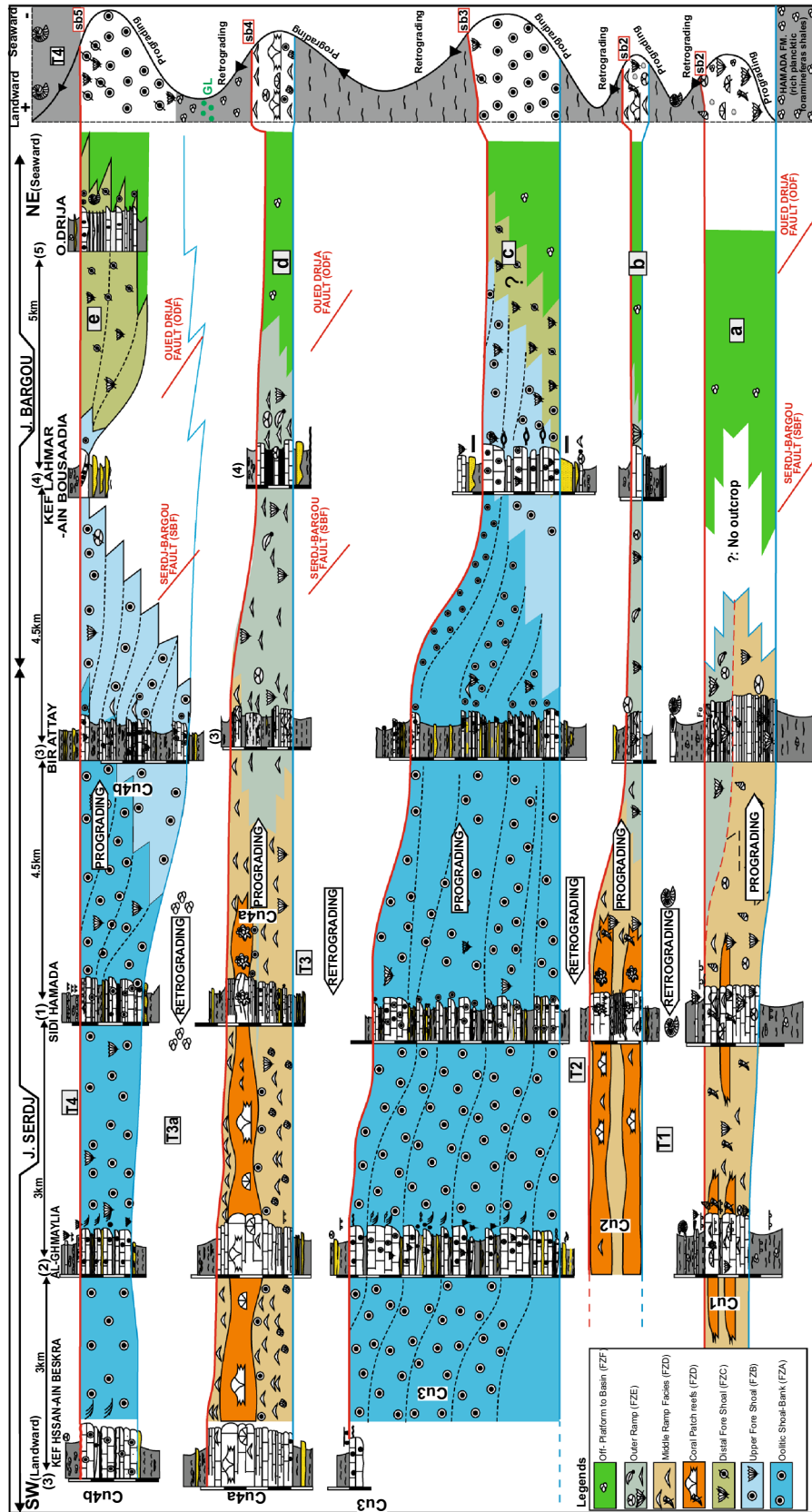


Fig. 16 Detailed correlations between the logged sections of the Serdj-Bargou area of the Serdj-Bargou area of the main shallow-marine carbonate units (Cu1 to Cu4) with the dominant facies associations (see Table 1). These correlations show that the Lower Serdj carbonate platform formed over several phases (platforms) separated by transgressive units (Heldt et al., 2010). The carbonate units clearly show a northward facies and thickness decrease, demonstrating that the proximal parts of these platforms are located at Jebel Serdj (middle and southern part) and their distal parts located to the north (Jebel Bargou). This explains that most of these carbonate units were already prograding to the north whereas the terrigenous units may correspond to distal parts or retrograding platforms which are situated south of Jebel Serdj

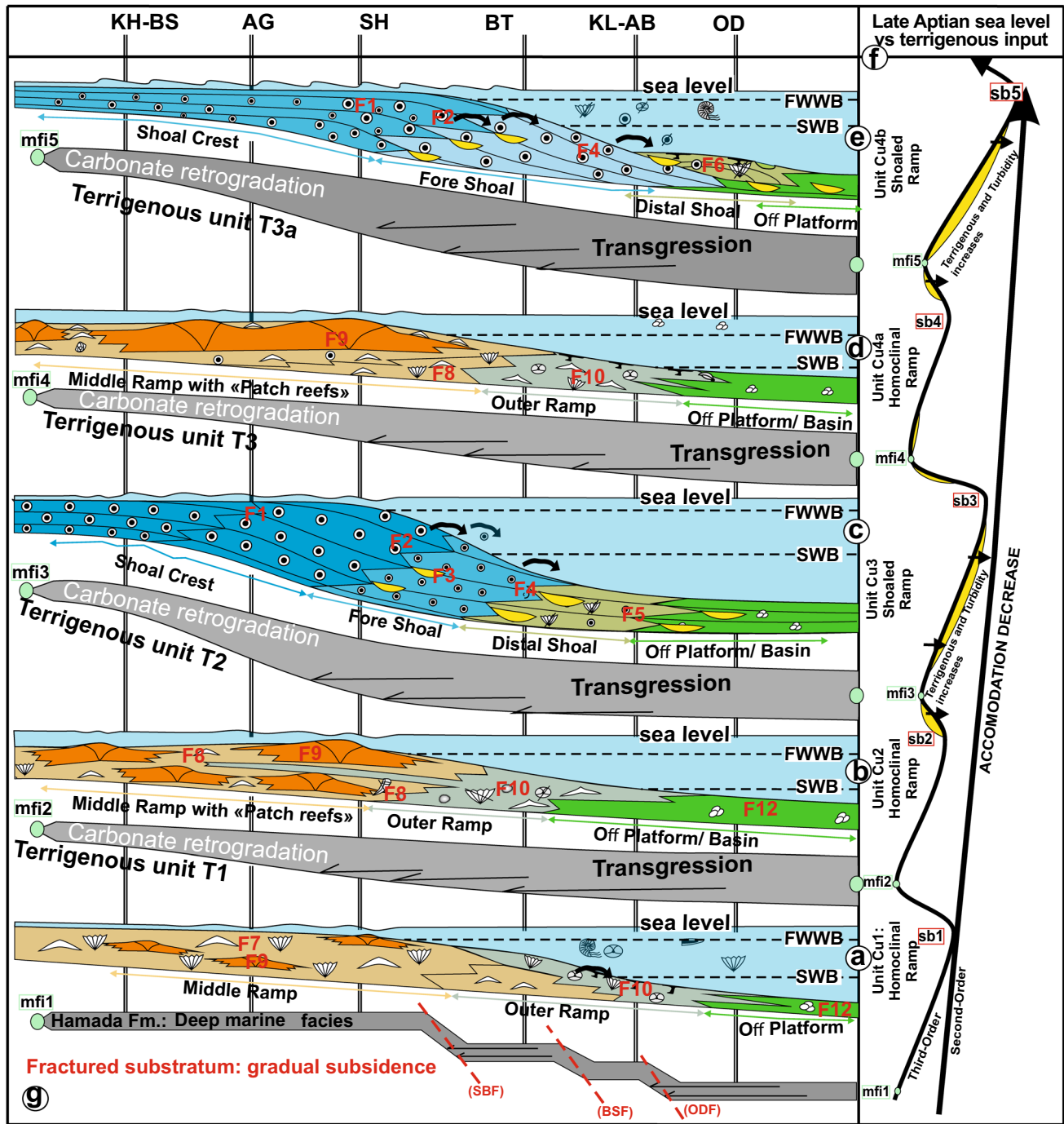


Fig. 17 Depositional models of the main late Aptian carbonate events (units Cu1 to Cu4) of the Serdj-Bargou area. **a** The first unit (Cu1) was deposited on a mid to outer homoclinal ramp. **b** The second unit was deposited on a mid to outer homoclinal ramp with common coralline buildups. **c** This stage corresponds to the unit Cu3 where sedimentation took place within a shoaled distally steepened ramp, with thickest oolitic facies present at jebel Serdj. **d** This stage corresponds to unit Cu4a deposited on a mid homoclinal ramp system with common small buildups on the Al-Ghamaylia-Sidi Hamada transect. The

facies at the BT and KL sections represent an outer ramp setting. **e** The last shallow-marine unit Cu4b developed within a shoaled ramp system. The proximal part of these platforms is situated at jebel Serdj and its distal parts are located in the Oued Drija area. **f** Deduced sea-level curve based on facies analysis of Ben Chaabane et al. (2019, Fig. 14). The average amount of sand has played a key role in the sedimentation from one platform to another. **g** Tectonic control and the main faults active during the late Aptian period and influencing the vertical and lateral sedimentation patterns

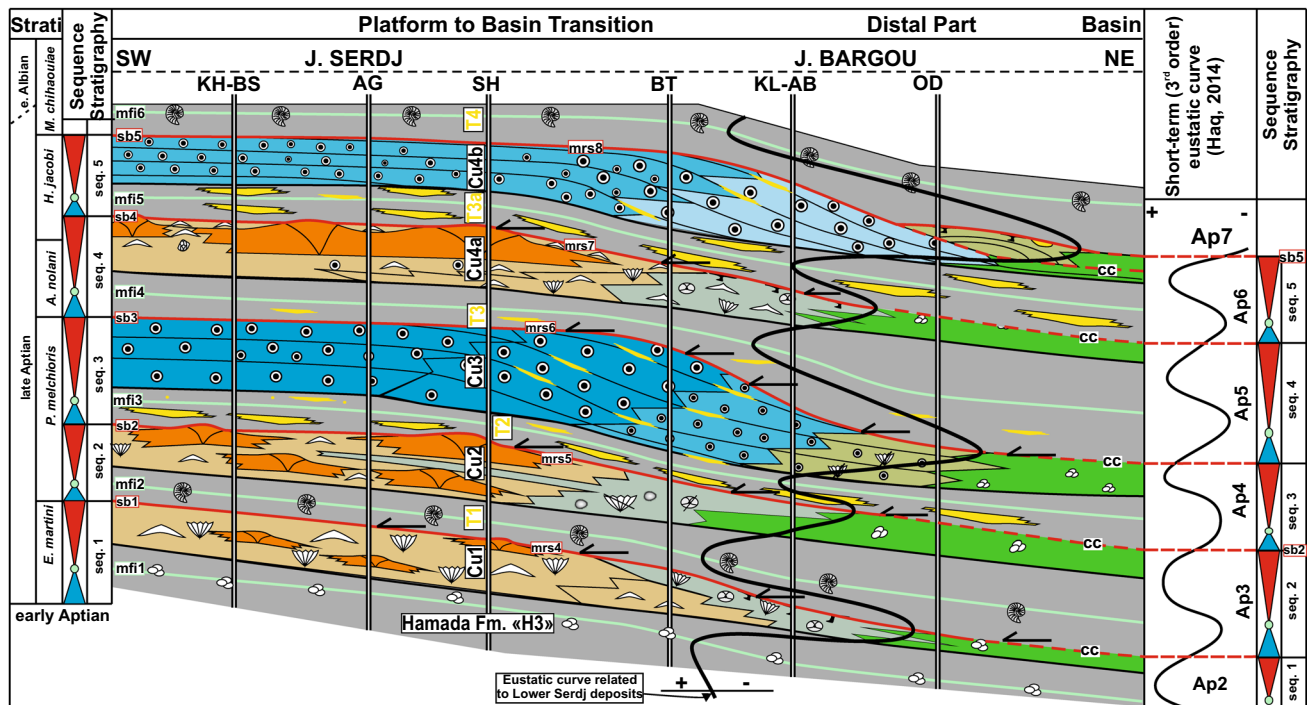


Fig. 18 Schematic chart summarizing facies and geometrical patterns of the late Aptian strata (Lower Serdj Formation) with the main third-order sequence stratigraphy. This chart illustrates the relative influence of eustatic sea-level variations which is clearly in concordance

with the third-order sea-level cycles of Haq (2014) at the Tethyan domain. The reconstructions have been made based on the environmental interpretation of the facies, biostratigraphically controlled by ammonites (Ben Chaabane et al. 2019)

For the AG and SH sections at jebel Serdj, sedimentation was mostly dominated by high-energy facies (80–90 thick), represented by abundant oolitic deposits, forming repetitive shallowing and shoaling-upward parasequences with a high terrigenous content (Fig. 5a). These parasequences begin with silty marl containing lenticular sandstones passing up into sandy cross-bedded oolitic limestones (Figs. 5a, 16c). The dominant textures are oolitic grainstone and oo-bioclastic grainstone/packstone (Table 1). Ooids are well-rounded with nuclei mostly of quartz grains (Fig. 6c, d). In this case, sedimentation took place within a Shoal Crest environment (facies F1 and F2 of the zone FZ A).

The features of this zone indicate a tide-dominated shallow-water environment devoid of oligotrophic indicators (Heldt et al. 2010). Oolite facies typically occur near the seaward edge of platforms, on banks, and the inner parts of ramps (Burchette and Wright 1992; Strasser and Vedrine 2009; Flügel 2010). Here it was under a terrigenous influence that the ooids developed. The presence of coral, bryozoan and rudist fragments suggests minor transportation and reworking (Fig. 6).

Towards the BT section, the Cu3 records a net thickness decrease to 60 m thick. Moreover, the oolite-dominated bodies show a progressive decrease in thickness

(Figs. 5b, 16c) and facies change. However, there is a significant thickness increase for intra-Cu3 shaly units. At jebel Bargou (KL-AB), the deposits of the Cu3 unit are mainly represented by cross-laminated lenticular limestone bodies (35 m thick) with medium to poorly sorted oolites and common parallel lamination, hummocky cross-stratification and trough cross-bedding (F4). At jebel Bargou, most of the oolitic bodies show well-preserved prograding features. The main observed textures are oolitic grainstone and graded wackestone, associated with aggregates, bioclasts, echinoderms debris and rare orbitolinids. Allochthonous material (Fig. 8c, d) was transported from the southern parts of the study area. Thus, it is suggested that the BT and KL-AB sections are dominated by “Fore Shoal” facies (Figs. 7, 17c) influenced by a storm waves, as indicated by the presence of HCS at the KL-AB section (Figs. 5d, 8).

Stage 4, Cu4a carbonate unit

This stage is characterized by high carbonate productivity with the development of biostromal buildups (Fig. 14a). The carbonates of this unit show net northward facies and thickness changes. The biota is dominated by corals, orbitolinids, miliolids, gastropods and oysters, reflecting the oligophotic

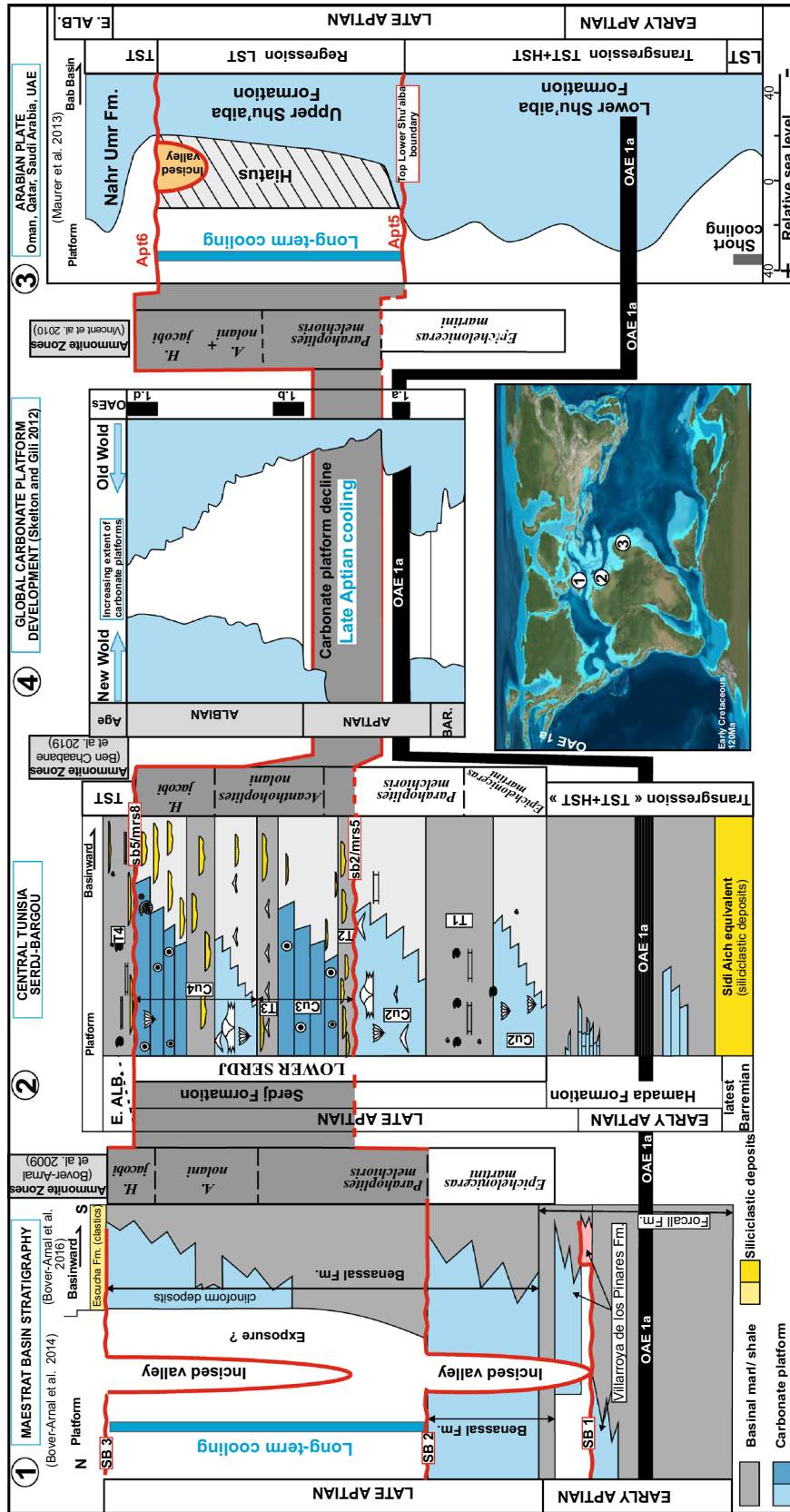


Fig. 19 Bio-chronostratigraphic correlation of three schematic sections (1: Iberian plate, 2: Tunisia and 3: Arabian plate) around the Tethyan domain for the Aptian sedimentary record. The age calibration is based on Tethyan ammonite zonation and Oceanic Anoxic Event 1a “OAE 1a” (Van Buchem et al. 2010; Bover-Arnal et al. 2014, 2016; Reboulet et al. 2014; Ben Chaabane et al. 2019). This correlation highlights the late Aptian global regression represented here in dark grey colour and bracketed between two bold red lines

conditions on a homoclinal carbonate ramp (Figs. 10c, 13b, c, 16d, 17d) occasionally influenced by waves. Several environments can be distinguished: FZ D and FZ E and FZ F. The FZ D zone is composed of two facies in the SH section and the southern part of Jebel Serdj (KH-BS and AG sections). The first one (F7) is represented by well-bedded oo-bioclastic limestones. These limestones consist of mud-coated grain (or pseudo-oolites) and orbitolinid grainstone, bioclast and miliolid-rich wackestone and orbitolinid grainstone (F8). The F7 and F8 facies represent a moderate energy environment, and they are present in the lower part of Cu4a (10–15 m thick; Fig. 12e, f). The F9 facies comprises well-preserved corals associated with common oysters, gastropods, annelids and orbitolinids (Fig. 12). This facies of FZ E consists of several coralline “biostromes” (10–15 m thick), of a subtidal relatively open-marine area (Fig. 10c). All these facies were deposited on a middle homoclinal ramp (FZ D) with patch reefs (Table 1) developed above some very local palaeo-highs. The facies zone FZ F of this stage is identified at the BT and KL-BS section (15–25 m thick). It is mainly represented by an alternation (Fig. 13b, c) of orbitolinid-rich, echinoderm, oyster, brachiopod marls with well-bedded bioclastic limestones and common bioturbation, especially within the marls (F11). This facies represents an outer homoclinal ramp environment with low energy (Figs. 16d, 17d), sporadically affected by storm waves.

Stage 5, Cu4b carbonate unit

This carbonate event took place after the sandy transgressive unit (T3a), including the mfi5 (mfs7 of Ben Chaabane et al. 2019), and is capped by sequence boundary sb5 (Fig. 10d, e Mrs8 of Ben Chaabane et al. 2019). The central oolitic bodies show a progressive northward thickness decrease, towards the BT section (Figs. 16e, 17e). Furthermore, they indicate that the southern part of Jebel Serdj was dominated by tidal activity, creating the thickest shallow-water facies (FZ A: F2), which prograded northwards, toward the subsiding basin (Oued Drija).

At the BT section, the oolitic-rich facies are commonly associated with lumachelle orbitolinid-oyster tempestites (F4). For Jebel Bargou (KL-AB section), the Cu4b deposits are only represented by one limestone unit (6 m thick) composed of cross-laminated, lenticular, medium to poorly sorted oolitic grainstone/wackestone with common aggregates and shell debris (F5). The facies Cu4b at the BT and KL-AB sections were deposited within a “Fore Shoal” environment (Fig. 17e).

Northwards, at the Drija locality, the Cu4b oolitic facies (18 m thick) are represented by discontinuous lenses displaying parallel plane lamination. Most of the oolitic lenses associated with the graded bioclastic tempestites and thin fine sandstones are interbedded with shale (Fig. 9a, b). The

bioclastic tempestites contain common glauconite which likely formed during sediment starvation (Wilson 1975; Flügel 2010), and ooids are mostly mud-coated, indicating a low-energy setting (Fig. 9f). All of these features suggest sediment derived from reworking of the shoal complex (Serj-Bargou) then re-deposition at Drija in a distal shoal setting. The laterally dominant oolitic facies arrangement of both Cu 3 and Cu4 is comparable to the well-documented upper Jurassic oolitic Iberian shoaled-ramp systems of the northern margin of the Tethyan realm (Aurell et al. 1998; Qi et al. 2007; Alnazghah et al. 2013; Pomar et al. 2015).

Terrigenous units T1, T2, T3, T3a and T4 (Fig. 15)

All of the terrigenous units show important thickness increases from south to north with some facies changes (Ben Chaabane et al. 2019; Ben Chaabane 2019). They are here included within the Facies Zone FZ G. Facies F12 is identified for T1 and T3 deposits. The T1 terrigenous unit (65–80 m thick) overlies the Cu1 carbonates and is mainly composed by green to grey shale and marl with interbedded nodular decimeter-thick bioclastic limestones (0.3–0.8 m of thick) rich in ammonites and belemnites in the central part. The T3 unit is 10 to 25 m thick and is mainly composed of shale and marl rich in ostracods, orbitolinids and planktic foraminifera, with interbedded orbitolinid-rich nodular limestone and sandstone with parallel lamination (0.2–0.7 m thick). The terrigenous units T2 (25–40 m thick) and T3a (20–40 + m thick) are mainly composed of an alternation of green silty marl and sandstone beds (0.2–1 m thick) with common sedimentary structures (parallel stratification, ripple marks and HCS). They are interpreted as offshore storm-affected sandstones and are included within the F13 facies.

Discussion

Lower Serdj Formation sedimentation was affected by significant intermittent terrigenous input that resulted in the installation in Central Tunisia of a mixed carbonate–siliciclastic system and a multi-phased carbonate platform. The migration of facies belts in the region (prograding and retrograding) was controlled by the interplay of tectonics, sea-level oscillations, terrigenous input and climate.

Tectonics and basin structure

In the Tethyan realm, the late Aptian period was characterized by regional extensional and sinistral transtensional tectonics (Buroillet and Ellouze 1986; Turki 1985;

Ricou 1994; Bouaziz et al. 2002; Ouahchi et al. 2003; El Euch 1990; Rigane et al. 2010). In the Serdj-Bargou area, sedimentation took place at a time of tectonic activity creating a pattern of episodic palaeo-highs and lows. This configuration provided the ultimate conditions for shoal and patch-reef development (Figs. 1, 17g). A north-dipping slope, controlled by episodic tectonic instabilities, established an upward-shoaling distally steepened ramp with major oolitic shoals. This tectonic configuration was affected by the reactivation of palaeo-faults including the E–W Serdj-Bargou fault (SBF), Bousadia fault (BSF) (Turki 1985), and the NW–SE Drija fault system (ODF) (Figs. 1, 3a, 17g). However, the Drija domain was the most subsident area during the Late Aptian. Halokinetic movements also enhanced uplift of the *jebel Serdj* area where the oolitic shoals were developed. During periods of tectonic stability, seafloor topography was reduced producing a gentle slope such that the oolitic shoaled ramp facies developed into a homoclinal ramp facies with common patch reefs. Strasser and Vedrine (2009) and Rankey and Reeder (2011) interpreted shoal facies as most likely developed on seabed topographic palaeo-highs that allowed the development of oolitic-bioclastic facies.

Sea-level oscillations and platform evolution

The Lower Serdj Formation exhibits progradational, aggradational and retrogradational geometries reflecting net changes in accommodation space (Figs. 16, 17f) on the scale of second and third-order cycles (Hardenbol et al. 1998; Catuneanu et al. 2011; Catuneanu 2019; Ben Chaabane et al. 2019). Herein, the established sequence-stratigraphic model proposed for the LSF deposits (Fig. 18) highlights the internal stratigraphic architecture and sedimentary elements of the various events (Fig. 18). Within the platform-to-basin transect (Ben Chaabane et al. 2015), a full spectrum of facies and palaeo-environments is represented, and platform stages are well-displayed in the field (Table 1, Fig. 16). Each carbonate platform stage of the LSF followed a transgressive unit and is bounded at the top by a sequence boundary (sb/Mrs) (Figs. 5, 18). These boundaries (sb1 to sb5) separate the dominantly shallow-marine carbonates (Cu1 to Cu4) from the mixed shale–siliciclastic–limestone transgressive units (T1 to T4) that include the maximum flooding intervals (mfi). These key surfaces define third-order cycles (Jacquin et al. 1991; Pomar et al. 2015; Catuneanu 2019; Ben Chaabane 2019).

The LSF platform carbonate packages occupied different geographical positions through time, with each

shallow facies break being more basinward, with the oolitic grainstones the most regressive and progradational units. However, the stages dominated by corals and orbitolinids (Cu2 and Cu4a) were deposited within more open-marine settings. Consequently, the most regressive surfaces are recorded at the top of the two oolitic units (sb3 and sb5) with net regression accompanied by northward facies progradation in response to the net decrease of accommodation space (Figs. 17, 18). The presence of some organisms in their life position, such as corals and sponges, trapping micritic and clayey sediment within the Cu2 and Cu4a carbonate units, reflects the increase in accommodation space and more moderate energy compared to the oolitic facies (Cu3 and Cu4a) (Tomás et al. 2013; Alnazghah et al. 2013; Pomar et al. 2015). Andres et al. (2006) related the growth geometries of modern marine buildups from back-shoal lagoonal environments in the Exumas, Bahamas, both to the accommodation space availability and appropriate water energy.

In summary, the late Aptian short-term sea-level rises and falls have greatly controlled the facies distribution and the internal architecture of the LSF (Figs. 16, 18). The Hamada and LS formations constitute a second-order cycle where the maximum regressive surface (sb5) is recorded at the top of the oolite unit of the Cu4b (Fig. 17). Thus, a net accommodation decrease is recorded from the base to the top of these LS deposits (Fig. 16). In fact, a clear downstepping of the shoal basinward has been observed and is recorded by the reworking and re-sedimentation of the thin oo-bioclastic beds in the Drija area.

Siliciclastic input implications and vertical facies evolution

Moving from the upper Hamada Formation to the LSF (Figs. 1b, 2), sedimentation passed from pelagic deep-marine deposits (H3; Fig. 2) to shallow-marine deposits (Cu1). This transition is well expressed, at a global scale, by a negative oxygen isotope excursion. It has been identified from mid-Late Aptian deep-sea carbonates on the Exmouth Plateau, NW Australian margin (Clarke and Jenkyns 1999), the southern and the northern Tethyan margins such as the Prebetic domain and Galve (Maestrat Basin) on the Iberian plate (e.g., Bover-Arnal et al. 2016; Skelton et al. 2019). Furthermore, Lehmann et al. (2009) identified this isotopic signature within the Aptian deposits of Central Tunisia. The isotope stratigraphy of the mid-Late Aptian has been interpreted as a consequence of global warming interrupted by sharp cooling events (Heldt et al. 2010; Bonin 2011; van Buchem et al. 2010).

The late Aptian time in Central Tunisia was characterized by high siliciclastic input (Tlatli 1980; Heldt et al.

2010; Ben Chaabane 2019). For the LSF, the siliciclastic units (Fig. 15) are T2, T3, T3a and T4, and followed by the oolitic deposits of the Cu3 and Cu4b units (Figs. 4, 5, 18). An increase in water turbidity due to these high siliciclastic influxes (Figs. 15, 17f) can be invoked to explain the vertical facies variations from one depositional stage to the next (Fig. 17). This water turbidity increase and transparency reduction decreased the lower limit of light-penetration and contracted the photic zones (Morsilli et al. 2012). This could explain the decline of benthic autotrophic and mixotrophic organisms, including corals, sponges and orbitolinids, during some stages (Fig. 17). In addition, the terrigenous input would have reduced the total calcium, and consequently impacted the carbonate productivity of some reefal and benthic communities (Hallock and Schlager 1986). Thus, the limestone units Cu2 and Cu4a (Fig. 17) were confined to deeper water when the clastic deposition retreated landwards during sea-level rise. Clearer water and increased light allowed the growth of carbonate producers, whereas for Cu3 and Cu4b higher energy led to oolitic deposits. Increased terrigenous runoff also brings higher nutrient supply (phosphorus, nitrogen, organic matter in suspension) which could have decreased the light intensity in the water column (Olivier et al. 2004, 2008; Gréselle and Pittet 2005). This would also have directly impacted the biotic responses of the main shallow-marine carbonate stages (Morsilli et al. 2012; Hallock and Schlager 1986).

The coral buildups of the Cu2 and Cu4a (rarely for Cu1) carbonate stages pass laterally, basin-ward, to bioclastic and orbitolinid facies (F11). The carbonate stages dominated by metazoan organisms and orbitolinids contain metre-thick massive coralline biostromes for the Cu1, Cu2, and Cu4a (Fig. 17a–d), located in the middle and southern parts of *jebel Serdj* (AG–SH sections). In this area, there would likely have been little influence of terrigenous material (Fig. 18), favouring biotic growth in the mesophotic to oligophotic zone, under the warm climate in well-oxygenated and clear water (Margalef 1968; Fries et al. 1984; Hallock 1986; Weissert et al. 1998; Strasser et al. 1999; Simmons et al. 2000; Wortmann et al. 2004; Olivier et al. 2004; Morsilli et al. 2012). The localized development of limestone units Cu2 and C4a was likely related to periodic terrigenous input (T2 and T3a; Fig. 18) and possibly to short periods of humid climate. The increase in terrigenous input is generally unfavourable for an oligotrophic biota. Some authors (e.g., Heldt et al. 2010; Bonin 2011; van Buchem et al. 2010; Maurer et al. 2013) have suggested an episode of intensified greenhouse conditions during the Aptian might have increased fluvial runoff and nutrient transfer rates.

Furthermore, the Cu3 and Cu4b carbonate units occur above the two terrigenous units, respectively, T2 and T3a;

they contain sandstone beds and most of the ooids have a quartz nucleus (Figs. 5, 6). The lack of oligotrophic bioclasts in these oolites could be due to the high siliciclastic input preventing benthic organisms (Heldt et al. 2010; Ben Chaabane et al. 2019) such that only oolite-rich facies were deposited. The effect of turbid waters following units T2 and T3a, accompanying relatively high siliciclastic runoff, may also explain the vertical facies pattern of coral-dominated to oolite-dominated facies (Figs. 16, 17, 18). This increased siliciclastic runoff suggests humid-pluvial conditions for this area in Tunisia, as have been invoked for other Tethyan domains (Weissert et al. 1998; Wortmann et al. 2004; van Buchem et al. 2010; Föllmi 2012; Maurer et al. 2013).

Global significance of the Tunisian late Aptian sedimentary record

The input of terrigenous material and formation of thick shallow-marine oolites, after an open platform rich in corals and orbitolinids, needs an explanation. It corresponds, probably, to an interval of widespread forced regression detected in several localities around the world, including (1) the Russian platform, leading to widespread erosion and sedimentation limited to subsident areas (Sahagian et al. 1996), (2) Western Siberia (Medvedev et al. 2011) and Western Canada (Zaitlin et al. 2002) where several Late Aptian incised valleys and associated clastic fills have been described, and (3) in the Tethyan domain: Iberia (Rodríguez-Lopez et al. 2008; Bover-Arnal et al. 2012, Bover-Arnal et al. 2014), the Apennines of southern Italy (Graziano and Raspini 2015) and the Arabian plate (Gréselle and Pittet 2005; Van Buchem et al. 2010; Maurer et al. 2010, 2013).

The early to late Aptian Shu'aiba Formation of Oman-Qatar-Saudi Arabia (Fig. 19-3), capped by the Apt5 sequence boundary (Al-Husseini and Matthews 2010; van Buchem et al. 2010), records the development of incised valleys, at the time of the Apt5 boundary, filled by clastics in the latest Aptian (Pierson et al. 2010; Maurer et al. 2010). The time gap represents a 5 million-year long hiatus including the *Parahoplites melchioris*, *Acanthohoplites nolani* and *Hypacanthoplites jacobi* ammonite Zones (Vincent et al. 2010), limited at the base by the Apt5 and at the top by the Apt6 sequence boundaries (Fig. 19-3). Laterally in the proximal setting (Bab Basin), the same period is recorded in lowstand clinoform deposits of the Upper Shu'aiba Formation (Gréselle and Pittet 2005; Maurer et al. 2010; Al-Husseini and Matthews 2010; van Buchem et al. 2010). Later, Maurer et al. (2013) postulated that this pronounced regressive period coincides with a long-term cooling event that promoted up-dip platform erosion and incision.

For the Iberian plate, Bover-Arnal et al. (2014) deduced that a normal lowstand systems track with clinofolds was deposited in the late Aptian in an inner platform subsident area (Fig. 19-1) in the northern part of the Maestrat Basin (Fig. 11; sb2). A major late Aptian sea-level fall is recorded by a 90-m-deep incision into a Lower Aptian carbonate platform in the Maestrat basin (Bover-Arnal et al. 2014). This sequence boundary sb2 (Fig. 19) marks the lowest point of relative sea level and thus the time of least accommodation space in the Aptian, with the only space for sedimentation still available being on the slopes and in the basins.

Moving to the southern Tethyan margin and according to Ben Chaabane et al. (2019), the Aptian deposits (Hamada and Lower Serdj deposits) form a second-order cycle. Furthermore, the T2, Cu3, T3 and Cu4 units, where the shallowest-water oolitic facies and the highest terrigenous influx are recorded, have been assigned to the last half of the late Aptian, based on the ammonite zones *Parahoplites melchioris*, *Acanthohoplites nolani* and *Hypacanthoplites jacobi* (Latil 2011; Reboulet et al. 2014; Ben Chaabane et al. 2019; Fig. 19). Herein, the stacked facies reveal third-order depositional sequences that record a gradual shallowing in the upper part (top Cu4b: sb5; Figs. 10d, e, 17, 18, 19). Also in these Late Aptian deposits, an increase in terrigenous input is recorded (Figs. 15, 18) and the occurrence of the shallowest-water facies (FZ A, FZ B and FZ C). These are bracketed by two sequence boundaries, sb4 and sb5 (Fig. 18). Hence, this succession coincides with a clear decrease in accommodation space (Fig. 17) with subaerial exposure (Fig. 10d, e; sb5), at the top of Cu4b (Figs. 17, 18, 19). It is suggested that the successive subaerial exposure of the up-dip domains of the late Aptian carbonate platform in southern and central Tunisia (Ben Chaabane et al. 2019) led to widespread erosion and, moreover, to siliciclastic sedimentation in proximal settings, such as the Serdj-Bargou domain. Thus, the terrigenous beds located within the Lower Serdj Formation of this domain, especially those situated between sb2 and sb5 sequence boundaries, may represent the products of these erosion episodes. Furthermore, the latest Aptian transgressive terrigenous unit T4 (Figs. 4, 18), following the sb5 boundary, is probably coeval in age to the siliciclastic backfills of the late Aptian incised valleys (Fig. 19) observed in Qatar (Raven et al. 2010), western Siberia (Medvedev et al. 2011) and Iberia (Bover-Arnal et al. 2014).

Lastly, the Lower Serdj deposits along a platform to basin transect are dominated by the shallowest-water facies of the Aptian period and include several terrigenous units in its upper part. This has been compared with the above examples from Late Aptian successions around the Tethyan domain (Fig. 19) and other basins located in different latitudes, indicating a global significance. All this indicates that large parts of the Tethyan and other

margins were subaerially exposed during the Late Aptian (Rodríguez-Lopez et al. 2008; Bover-Arnal et al. 2012; Maurer et al. 2013) and their basin-ward equivalent strata correspond to lowstand systems track deposits, such as present in the Tunisian Lower Serdj Formation, the Upper Shu'aiba Formation of the Arabian plate and the Benassal Formation on the Iberian plate.

Moreover, Skelton and Gili (2012) (Fig. 19-4) proposed climatic changes, involving cooling and southward movement of a humid climatic belt across Iberia (Bover-Arnal et al. 2010, 2016) and the Arabian plate (Maurer et al. 2013) and, herein, Tunisia. These humid conditions were likely the main factor behind the demise or decline of some late Aptian carbonate platforms (Fig. 19). These late Aptian climatic conditions clearly influenced LSF sedimentation and carbonate production. It resulted in periodic suppression of biogenic carbonate production, especially when a dominant coral–rudist–sponge association was replaced by ooid-rich facies with siliciclastic input. Consequently, these data, that document a long-term reduction in accommodation space, fit well with the global regression and cooling recognized in several basins worldwide, and support a glacio-eustatic interpretation (Gréselle and Pittet 2005; van Buchem et al. 2010; Skelton and Gili 2012; Raven et al. 2010; Bover-Arnal et al. 2014). To confirm this global impact, a glaciation of Antarctica needs to be found, and glacier formation in lower latitudes and at high altitudes not neglected (Maurer et al. 2010, 2013; Bover-Arnal et al. 2014).

Conclusions

The Serdj-Bargou area of Central Tunisia exhibits excellent outcrop sections along a NE–SW km-scale transect for the examination of a late Aptian shallow-marine carbonate system. The primary outcomes of the work undertaken in this area are

- (1) During the late Aptian period, five shallow-marine carbonate stages are recognized within a mixed carbonate–siliciclastic succession. Transgressive terrigenous units separate these shallow-marine carbonates with a variable siliciclastic input from one stage to another.
- (2) Several facies have been identified and assembled into facies zones to understand the partitioning and distribution of the main facies that comprise the five dominant-carbonate stages. The established depositional models show changes from a coral-orbitolinid (with rudists and sponges) homoclinal ramp system for Cu1, Cu2 Cu4a to an oolite-dominated distally steepened ramp system for Cu3 and Cu4b.

- (3) The lateral facies belt migration (progradation and retrogradation) and their vertical stacking within the LSF mixed siliciclastic–carbonate system reflect the interplay of several factors.
- (4) Third-order sea-level fluctuations controlled the LSF mixed siliciclastic–carbonate platform internal architecture. The carbonate stages of the LSF were deposited during the regressive systems track, with the decrease in accommodation space impacting the facies distribution for each carbonate stage.
- (5) This work supports earlier interpretations that periodic siliciclastic input is related to short-lived climatic perturbations, which strongly influenced shallow-marine carbonate production, notably through increased turbidity and nutrient supply.
- (6) Previous global eustatic and climatic models applied to the late Aptian are supported by the Lower Serdj sedimentary record documented here from Tunisia and concur with the glacio-eustatic interpretation of late Aptian global regression.

Acknowledgements This paper is a part of the first author's PhD thesis (LR18ES07, Department of Geology, Faculty of Sciences, University of Tunis El Manar). We would like to thank the Tunisian Oil Company (ETAP) for providing the logistical support for this project. We are grateful to the Editor-in-Chief Maurice Tucker and to Bernard Pittet and J Josep A. Moreno Bedmar, for their extremely helpful comments and detailed reviews that greatly improved the original manuscript. We are grateful to Dr. D. J. Salmouna for the English revision that improved the quality of the first draft of the manuscript. The first author of this work warmly thanks Dr. Robert W. Scott from Oklahoma University (USA) who provided valuable comments and corrections to the early version of the manuscript. Assistance in the field by H. Sayari, A. Hedfi and A. Bechellaoui are very much appreciated.

Author contributions NBC led the research as well as detailed knowledge on the research target and discussions. NBC wrote the manuscript and created the figures. NBC and FK logged the field sections. FK greatly improved the manuscript and the figures during the revision round, and aided fieldwork planning and logistics. MS contributed significantly to the first steps of scientific progress of the research. IBHT provided knowledge on some stratigraphic questions. All the authors contributed to insightful discussions that formed this article.

References

- Al-Husseini MI, Matthews RK (2010) Tuning Late Barremian–Aptian Arabian Plate and global sequences with orbital periods. *GeoArabia Spec Publ* 4:199–228
- Alnazghah MH, Bádenas B, Pomar L, Aurell M, Morsilli M (2013) Facies heterogeneity at interwell-scale in a carbonate ramp, Upper Jurassic, NE Spain. *Mar Pet Geol*. <https://doi.org/10.1016/j.marpetgeo.2013.03.004>
- Andres MS, Sumner DY, Reid RP, Swart PK (2006) Isotopic fingerprints of microbial respiration in aragonite from Bahamian stromatolites. *Geology* 34:973–976
- Aurell M, Bádenas B, Bosence DWJ, Waltham DA (1998) Carbonate production and offshore transport on a Late Jurassic carbonate ramp (Kimmeridgian, Iberian basin, NE Spain): evidence from outcrops and computer modelling. In: Wright VP, Burchette TP (eds) *Carbonate ramps*, vol 149. Geol Soc London Spec Publication, pp 137–161
- Ben Chaabane N (2019) Aptian–Early Albian carbonate platform development of Serdj Bargou and adjacent domains (Atlas Tunisia): surface–subsurface stratigraphy; sedimentology and depositional models; sequence stratigraphy and reservoir characterization. Thesis on geologic sciences (unpublished). University of Tunis El Manar, p 444
- Ben Chaabane N, Soussi M, Khemiri F, Troudi H, Ouahchi A (2013) Architecture des dépôts carbonatés de la bordure de plate-forme Serdj de la Tunisie centrale au Clansayésien (Aptien supérieur). *Association des Sédimentologues Français*, 2013. Volume des abstracts 28, p 250
- Ben Chaabane N, Khemiri F, Soussi M, Troudi H, Ouahchi A, Saidi M, Meskini A (2015) Aptian carbonate Platform of Central Tunisia: internal architecture and evolution. The 13 Conf. ETAP EPC 2015 (extended abstract)
- Ben Chaabane N, Khemiri F, Soussi M, Latil J-L, Robert E, Belhajtaher I (2019) Aptian–Lower Albian Serdj carbonate platform of the Tunisian Atlas: development, demise and petroleum implication. *Mar Pet Geol* 101:566–591. <https://doi.org/10.1016/j.marpetgeo.2018.10.036>
- Bonin A (2011) Relations entre les variations climatiques, les perturbations du cycle du carbone et les crises de la production. These en Science de la terre. Université de Bourgogne, France, p 242
- Bouaziz S, Barrier E, Soussi M, Turki MM, Zouari H (2002) Tectonic evolution of the northern African margin in Tunisia from paleostress data and sedimentary record. *Tectonophysics* 337:227–253
- Bover-Arnal T, Moreno-Bedmar JA, Salas R, Skelton PW, Bitzer K, Gili E (2010) Sedimentary evolution of an Aptian syn-rift carbonate system (Maestrat Basin, E Spain): effects of accommodation and environmental change. *Geol Acta* 8:249–280
- Bover-Arnal T, Salas R, Guimera J, Moreno-Bedmar JA (2014) Deep incision in an Aptian carbonate succession indicates major sea-level fall in the Cretaceous. *Sedimentology*. <https://doi.org/10.1111/sed.12105>
- Bover-Arnal T, Moreno-Bedmar JA, Frijia G, Pascual-Cebrian E, Salas R (2016) Chronostratigraphy of the Barremian–Early Albian of the Maestrat Basin (E Iberian Peninsula): integrating strontium–isotope stratigraphy and ammonoid biostratigraphy. *Newslett Stratigr* 49:41–68
- Burchette TP, Wright VP (1992) Carbonate ramp depositional systems. *Sed Geol* 79:3–57
- Burollet PF, Ellouze N (1986) L'évolution des bassins sédimentaires de la Tunisie centrale et orientale. *Bull Cent Rech Exploit Prod Elf Aquitaine* 10:49–68
- Catuneanu O (2019) Scale in sequence stratigraphy. *Mar Pet Geol* 106:128–159. <https://doi.org/10.1016/j.marpetgeo.2019.04.026>
- Catuneanu O, Galloway WE, StC Kendall CG, Miall AD, Posamentier HW, Strasser A, Tucker ME (2011) Sequence stratigraphy: methodology and nomenclature. *Newslett Stratigr* 443:173–245. <https://doi.org/10.1127/0078-0421/2011/0011>
- Clarke LJ, Jenkyns HC (1999) New oxygen isotope evidence for long-term Cretaceous climate change in the Southern Hemisphere. *Geology* 27:699–702
- Dunham RJ (1962) Classification of carbonate rocks according to their depositional texture. In: Ham WE (ed) *Classification of carbonate rocks*. A symposium, vol 1. American Association of Petroleum Geologists Memoir, Tulsa, OK, pp 108–121
- El Euch H (1990) La Tunisie du Centre-Ouest de l'Aptien à l'Actuel: tectonique coulissante, dynamique sédimentaire associée et

- essai de caractérisation des séquences de dépôt. Unpublished thesis, Doctorat 3ème cycle, Université Tunis II (Tunisia), p 263
- Fischer AG, Arthur MA (1977) Secular variations in the pelagic realm. *Soc Econ Paleontol Miner Spec Publ* 25:19–50
- Flügel E (2004) *Microfacies of carbonate rocks. Analysis, interpretation and application*. Springer-Verlag, Germany
- Flügel E (2010) *Microfacies of carbonate rocks, analysis, interpretation and application*, 2nd edn. Springer, Berlin, p 1006
- Föllmi KB (2012) Early cretaceous life, climate and anoxia. *Cret Res* 35:230–257
- Fries G, Beaudoin B, Joseph P, Paternoster B (1984) Les grès de Rosans et les slumpings aptiens associés: restitution paléomorphologique. *Bull Soc Geol France* 7:693–702
- Graziano R, Raspini A (2015) Long- and short-term hydroclimatic variabilities in the Aptian Tethys: Clues from the orbital chronostratigraphy of evaporite-rich beds in the Apennine carbonate platform (Mt. Faito, southern Italy). *Palaeogeogr Palaeoclimatol Palaeoecol* 418:319–343. <https://doi.org/10.1016/j.palaeo.2014.11.021>
- Gréselle B, Pittet B (2005) Fringing carbonate platforms at the Arabian Plate margin in northern Oman during the Late Aptian–Middle Albian: evidence for high-amplitude sea-level changes. *Sed Geol* 175:367–390
- Hallock P (1986) The role of nutrient availability in bioerosion: Consequences to carbonate buildups. *Palaeogeogr Palaeoclimatol Palaeoecol* 63:275–291. [https://doi.org/10.1016/0031-0182\(88\)90100-9](https://doi.org/10.1016/0031-0182(88)90100-9)
- Hallock P, Schlager W (1986) Nutrient excess and the demise of coral reefs and carbonate platforms. *Palaios* 1 89:398
- Haq BU, Hardenbol I, Vail PR (1988) Mesozoic and Cenozoic chrono-stratigraphy and cycles of sea-level change. In: Wilgus CK, Hastings BS, Kendall CGStC, Posamentier H, Ross CA, Van Wagoner JC (eds) *Sea level changes, an integrated approach*. Society of Economic Paleontologists and Mineralogists, Special Publication no 42, pp 71–108
- Hardenbol J, Thierry J, Farle MB, JacquiniGraciansky TDEPC, Vail PR (1998) Mesozoic and cenozoic sequence stratigraphy of European Basins. *SEPM Spec Public No* 60:1–13
- Heldt M, Lehmann J, Bachmann M, Negra MH, Kuss J (2010) Increased terrigenous influx but no drowning: palaeoenvironmental evolution of the Tunisian carbonate platform margin during the Late Aptian. *Sedimentology* 57:695–719
- Hfaiedh R, Vanneau AA, Godet A, Arnaud H, Zghal I, Ouali J, Latil J-L, Jallali H (2013) Biostratigraphy palaeoenvironments and sequence stratigraphy of the Aptian sedimentary succession at Jebel Bir Oum Ali (Northern Chain of Chotts South Tunisia): Comparison with contemporaneous Tethyan series. *Cretaceous Research* 46:177–207. <https://doi.org/10.1016/j.cretres.2013.08.004>
- Jacquini T, Arnaud-Vanneau A, Arnaud H, Ravenne C, Vail PR (1991) Systems tracts and depositional sequences in a carbonate setting: a study of continuous outcrops from platform to basin at the scale of seismic lines. *Mar Pet Geol* 8:122–139
- Latil J-L (2011) Early Albian ammonites from Central Tunisia and adjacent areas of Algeria. *Revue de Paléobiologie, Genève* 30:321–429
- Lehmann J, Heldt M, Bachmann M, Negra MEH (2009) Aptian (Lower Cretaceous) biostratigraphy and cephalopods from north-central Tunisia. *Cretac Res* 30:895–910
- M'Rabet A (1981) *Stratigraphie, sédimentation et diagenèse carbonatée des séries du Crétacé inférieur de Tunisie Centrale*. Thèse Doctorat ès Sciences, Université de Paris-Sud centre d'Orsay, p 540
- Margalef R (1968) The pelagic ecosystem of the Caribbean Sea: symposium on investigations and resources of the Caribbean Sea and adjacent regions. UNESCO, France, Paris, pp 484–498
- Masse JP (1984) Données nouvelles sur la stratigraphie de l'Aptien carbonaté de la Tunisie centrale, conséquences paléogéographiques. *Bull Soc Geol Fr* 6:1077–1086
- Masse JP, Bellion Y, Benkhelil J, Ricou LE, Dercourt J, Guiraud R (1993) Early Aptian (114–111 Ma). In: Dercourt J, Ricou LE, Vrielynck B (eds) *Atlas Tethys palaeoenvironmental maps*. Gauthier-Villars, Paris, pp 135–152
- Maurer F, Al-Mehsin K, Pierson BJ, Eberli GP, Warrlich G, Drysdale D, Droste HJ (2010) Facies characteristics and architecture of Upper Aptian Shuaiba clinofolds in Abu Dhabi. *GeoArabia Spec Publ* 4:445–468
- Maurer F, Van Buchem FSP, Eberli GP, Pierson BJ, Raven MJ, Larsen PH, Al-Husseini MI, Vincent B (2013) Late Aptian long-lived glacio-eustatic lowstand recorded on the Arabian Plate. *Terra Nov.* <https://doi.org/10.1111/ter.12009>
- Medvedev AL, Lopatin AY, Masalkin YV (2011) Comparative characteristics of the lithological composition of the incised valley fill and host sediments of the Vikulovo Formation, Kamenny Area, West Siberia. *Lithol Min Resour* 46:369–381
- Millán MI, Weissert HJ, Owen H, Fernández-Mendiola PA, García-Mondéjar J (2011) The Madotz Urganian platform (Aralar, northern Spain): paleoecological changes in response to Early Aptian global environmental events. *Palaeogeogr Palaeoclimatol Palaeoecol.* <https://doi.org/10.1016/j.palaeo.2011.10.005>
- Morsilli M, Bosellini FR, Pomar L, Hallock P, Aurell M, Papazzoni CA (2012) Mesophotic coral buildups in a prodelta setting (Late Eocene, southern Pyrenees, Spain): a mixed carbonate–siliciclastic system. *Sedimentology* 59(3):766–794. <https://doi.org/10.1111/j.1365-3091.2011.01275.x>
- Negra MH, Skelton PW, Gili E, Valdeperas FX, Argles T (2016) Recognition of massive Upper Cretaceous carbonate bodies as olistoliths using rudist bivalves as internal bedding indicators (Campanian Merfeg Formation, Central Tunisia). *Cretaceous Res* 66. <https://doi.org/10.1016/j.cretres.2016.06.003>
- Olivier N, Carpentier C, Martin-Garin B, Lathuilière B, Gaillard C, Ferry S, Hantzpergue P, Geister J (2004) Coral-microbialite reefs in pure carbonate versus mixed carbonate–siliciclastic depositional environments: the example of the Pagny-sur-Meuse section (Upper Jurassic, northeastern France). *Facies* 50:229–255. <https://doi.org/10.1007/s10347-004-0018-5>
- Olivier N, Pittet B, Werner W, Hantzpergue P, Gaillard C (2008) Facies distribution and coral-microbialite reef development on a low-energy carbonate ramp (Chay Peninsula, Kimmeridgian, western France). *Sediment Geol* 205:14–33. <https://doi.org/10.1016/j.sedgeo.2007.12.011>
- Ouahchi A, M'Rabet A, Lazreg J, Messaoudi F, Ouazza S (1998) Early structuring, paleo-emersion and porosity development: a key for exploration of the Aptian Serdj carbonate reservoir in Tunisia. In: *Proceedings of the 6th Tunisian petroleum exploration and production conference*, vol 6, Tunis (Tunisia), pp 267–284
- Ouahchi A, Abbassi K, El Euch H (2003) L'événement Aptien-Albien en Tunisie : mécanismes, structures associées et implications pétrolières. *ATEIG* 1:27–30
- Pierson BJ, Eberli GP, Al-Mehsin K, Al-Menhali S, Warrlich G, Droste HJ, Maurer F, Whitworth J, Drysdale D (2010) Seismic stratigraphy and depositional history of the Upper Shuaiba (Late Aptian) in the UAE and Oman. *GeoArabia Spec Publ* 4:411–444
- Pomar L (2001) Types of carbonate platforms: a genetic approach. *Basin Res.* <https://doi.org/10.1046/j.0950-091X.2001.00152.x>
- Pomar L, Hallock P (2008) Carbonate factories: a conundrum in sedimentary geology. *Earth Sci Rev* 87:134–169. <https://doi.org/10.1016/j.earscirev.2007.12.002>
- Pomar L, Kendall CG (2008) Architecture of carbonate platforms: a response to hydrodynamics and evolving ecology. *SEPM* 89:187–216

- Pomar L, Aurell M, Badenas B, Morsilli M, Fahd Al-Awwad S (2015) Depositional model for a prograding oolitic wedge, upper Jurassic, Iberian basin. *Mar Pet Geol* 67:556–582. <https://doi.org/10.1016/j.marpetgeo.2015.05.025>
- Qi L, Carr TR, Goldstein RH (2007) Geostatistical three-dimensional modeling of oolite shoals, St. Louis Limestone, southwest Kansas. *AAPG Bull* 91:69–96
- Rankey EC, Reeder SL (2011) Holocene oolitic Marine sand complexes of the Bahamas. *J Sediment Res* 81:97–117
- Raven MJ, van Buchem FSP, Larsen PH, Surlyk F, Steinhardt H, Cross D, Klem N, Emang M (2010) Late Aptian incised valleys and siliciclastic infill at the top of Shu'aiba Formation (Block 5, offshore Qatar). *GeoArabia Spec Publ* 4:469–502
- Read JF (1995) Overview of carbonate platform sequences, cycle stratigraphy and reservoirs in greenhouse and icehouse worlds. In: Read JF, Kerans C, Weber LJ, Sarg JF, Wright FM (eds) *Milankovitch sea-level changes, cycles and reservoirs on carbonate platforms in greenhouse and ice-house worlds*. SEPM short course, vol 35, pp 1–102
- Reboullet S, Szives O, Aguirre-Urreta B, Barragán R, Company M, Idakieva V, Ivanov M, Kakabadze MV, Moreno-Bedmar JA, Sandoval J, Baraboshkin EJ, Çağlar MK, Fozy I, González-Arreola C, Kenjo S, Lukeneder A, Raisossadat SN, Rawson PF, Tavera JM (2014) Report on the 5th international meeting of the IUGS lower cretaceous ammonite working group, the Kilian group (Ankara, Turkey, 31st August 2013). *Cretac Res* 50:126–137. <https://doi.org/10.1016/j.cretres.2014.04.001>
- Ricou LE (1994) Tethys reconstructed: plates, continental fragments and their boundaries since 260Ma from Central America to South Asia. *Géodyn Acta* 7:160–218
- Riding R (2002) Structure and composition of organic reefs and carbonate mud mounds: concepts and categories. *Earth Sci Rev* 58:163–231
- Riding R, Liang I (2005) Geobiology of microbial carbonates: meta-zoan and seawater saturation state influences on secular trends during the Phanerozoic. *Paleogeogr Paleoclimatol Paleoecol* 219:101–115
- Rigane A, Feki M, Gourmelen C, Montacer M (2010) The “Aptian Crisis” of the South-Tethyan margin: new tectonic data in Tunisia. *J Afr Earth Sc* 57:360–366
- Rodriguez-Lopez JP, Melendez N, de Boer PL, Soria AR (2008) Aeolian sand sea development along the mid-Cretaceous western Tethyan margin (Spain): erg sedimentology and palaeoclimate implications. *Sedimentology* 55:1253–1292
- Ross DJ, Skelton PW (1993) Rudist formations of the Cretaceous: a palaeoecological, sedimentological and stratigraphical review. *Sedimentol Rev* <https://doi.org/10.1002/9781444304534>
- Sahagian D, Pinous O, Olfieriev A, Zakharov V (1996) Eustatic curve for the Middle Jurassic-Cretaceous based on Russian platform and Siberian stratigraphy: zonal resolution. *Am Assoc Petrol Geol Bull* 80:1433–1458
- Sarg JF (1988) Carbonate sequence stratigraphy. In: Wilgus CK, Hastings BS, Kendall CGSC, Posamentier HW, Ross CA, Van Wagoner JC (eds) *Sea level changes—an integrated approach*. SEPM Special Publication, vol 42, pp 155–182
- Sedjil A (1981) Stratigraphie et Sédimentologie du Crétacé post-Aptien en Tunisie Centrale et Septentrionale. Thèse 3e Cycle, Univ. Paris-Sud. (Unpublished), p 141
- Simmons MD, Whittaker JE, Jones RW (2000) Orbitolinids from Cretaceous sediments of the Middle East—a revision of the F. R. S. Henson and Associates Collection. In: Hart MB, Kaminski MA, Smart CW (eds) *Proceedings of the fifth international workshop on agglutinated foraminifera*. Grzybowski Foundation Spec Publ 7, pp 411–437
- Skelton PW, Gili E (2012) Rudists and carbonate platforms in the Aptian: a case study on biotic interactions with ocean chemistry and climate. *Sedimentology* 59:81–117
- Skelton PW, Castro JM, Ruiz-Ortiz PA (2019) Aptian carbonate platform development in the Southern Iberian Aptian carbonate platform development in the Southern Iberian Palaeomargin (Prebetic of Alicante, SE Spain). *Bull Soc Geol France* 190:3. <https://doi.org/10.1051/bsgf/2019001>
- Soussi M (2002) *Le Jurassique de la Tunisie atlasique: stratigraphie, dynamique sédimentaire, paléogéographique et intérêt pétrolier*. Documents des laboratoires de Géologie de Lyon, p 363
- Strasser A, Vedrine S (2009) Controls on facies mosaics of carbonate platforms: a case study from the Oxfordian of the Swiss Jura. In: Swart PK, Eberli GP, McKenzie JA (eds) *Perspectives in carbonate geology: a tribute to the career of Robert Nathan Ginsburg*, pp 199–213
- Strasser A, Pittet B, Hillgartner H, Pasquier JB (1999) Depositional sequences in shallow carbonate-dominated sedimentary systems: concepts for a high-resolution analysis. *Sed Geol* 128:201–221
- Tlatli M (1980) *Etude des calcaires de l'apto-Aptien des Djebels Serdj et Bellouta (Tunisie Centrale)*. Thesis Aix-Marseille 2 Univ, p 187
- Tomás S, Homann M, Mutti M, Amour F, Christ N, Immenhauser A, Agar SM, Kabiri L (2013) Alternation of microbial mounds and ooid shoals (middle Jurassic, Morocco): response to paleoenvironmental changes. *Sediment Geol* 294:68–82. <https://doi.org/10.1016/j.sedgeo.2013.05.008>
- Touir J, Ben Haj Ali N, Donze P, Maamouri AL, Memmi L, M'Rabet A, Razgallah S, Zaghbib-Turki D (1989) *Biostratigraphie et sédimentologie des séquences du Crétacé supérieur du Jebel M'rhiba (Tunisie centrale)*. Géologie Méditerranéenne
- Troudi H (2000) Characterization of the Aptian Serdj Carbonate reservoir in the Kaboudia offshore Permit in Tunisia. *Planches internal report* 50, p 43
- Tucker ME, Wright VP (1990) *Carbonate Sedimentology*. Blackwell Scientific Publications, Oxford.
- Turki MM (1985) *Polycinématique et contrôle sédimentaire associé sur la cicatrice Zaghuan-Nebhana*. These Doct. es Sci. Université de Tunis, et *Revue des Sciences de la Terre*, Tunis, CST-NRST 7, p 252
- Van Buchem FSP, Al-Husseini MI, Maurer F, Droste HJ, Yose LA (2010) Sequence-stratigraphic synthesis of the Barremian – Aptian of the eastern Arabian Plate and implications for the petroleum habitat. *GeoArabia Spec Publ* 4:9–48
- Vincent B, van Buchem FSP, Bulot LG, Immenhauser A, Caron C, Baghbani D, Huc AY (2010) Carbon-isotope stratigraphy, biostratigraphy and organic matter distribution in the Aptian – Lower Albian successions of southwest Iran (Dariyan and Kazhdumi formations). *GeoArabia Spec Publ* 4:139–197
- Weissert H, Lini A, Follmi KB, Kuhn O (1998) Correlation of Early Cretaceous carbon isotope stratigraphy and platform drowning events. *Palaeogr Palaeoclimatol Palaeoecol* 137:189–203
- Wilson JL (1975) *Carbonate facies in geologic history*. Springer, New York, p 411
- Wortmann U, Herrle JO, Weissert H (2004) Altered carbon cycling and coupled changes in Early Cretaceous weathering patterns: evidence from integrated carbon isotope and sandstone records of the western Tethys. *Earth Planet Sci Lett* 220:69–82
- Zaitlin BA, Warren MJ, Potocki D, Rosenthal L, Boyd R (2002) Depositional styles in a low accommodation foreland basin setting: an example from the Basal Quartz (Lower Cretaceous), southern Alberta. *Bull Canad Petrol Geol* 50:31–72